The Pennsylvania State University

The Graduate School

Department of Materials Science and Engineering

MEASUREMENT OF CONDUCTING ION MOBILITY AND CONCENTRATION IN ION-CONTAINING POLYMERS

A Thesis in

Materials Science and Engineering

by

U Hyeok Choi

Submitted in Partial Fulfillment
of the Requirements
for the Degree of

Master of Science

December 2009

The thesis of U Hyeok Choi was reviewed and approved* by the following:

Ralph H. Colby
Professor of Materials Science and Engineering
Thesis Advisor

James Runt
Professor of Polymer Science

Qiming Zhang
Professor of Electrical Engineering and Materials Science and Engineering

Joan M. Redwing
Professor of Materials Science and Engineering
Chair, Intercollege Graduate Degree Program in Materials Science and Engineering

*Signatures are on file in the Graduate School

ABSTRACT

In this study, we focus on how to measure conducting ion mobility and conducting ion number density in ion-containing polymers. From a fundamental side, we do not yet understand how to design the ion-containing polymers to have a large and rapid ion response to an applied field. It is therefore necessary to develop precise measurement of number density and mobility of charge carriers. That can give rise to better understand the generation and transport processes of ionic carriers in these polymers. On the practical side, the fundamental performance characteristics make it possible to optimize the design of ion-containing polymers for advanced devices. We studied dielectric properties and ion conduction of poly(ethylene oxide) (PEO) based polyester copolymer ionomers, with and without crown ether, using dielectric relaxation spectroscopy. Addition of crown ether to PE600-0.5Li enhanced ionic conductivity. A physical model of electrode polarization enabled the ionic conductivity to be separated into conducting ion mobility and conducting ion concentration. The formation of Li-complex with crown ether causes a large increase in the static dielectric constant as well. The increase of the static dielectric constant boosts the number density of conducting ions, and this has the largest contribution to increased conductivity. In addition to the dielectric relaxation spectroscopy measurement, we suggested that a Hall Effect measurement may be able to directly measure both number density of conducting ions and their mobility even though the method has only been extensively used for the characterization of classical semiconductor materials. We defined and discussed fundamental equations of d.c. and a.c. Hall effect. Furthermore, the essential components of an apparatus for ionic Hall Effect measurements are investigated in several ionic systems. With these theoretical and experimental results, we tried to estimate Hall voltage of PE600-0.1Na using d.c. Hall Effect measurement.

TABLE OF CONTENTS

LIST OF FIGURES……vi

LIST OF TABLES……viii

ACKNOWLEDGEMENTS……ix

Chapter 1 Introduction and Motivation……1

1-1. Historical development of polymer electrolytes for ion transport……4

1-1.1. Plasticized polymer electrolyte……7

1-1.2. Poly(ethylene oxide)-based polymer electrolyte……8

1-1.3. Single ion conductors……10

1-2. Ion-conduction mechanisms in polymers……11

1-2.1. Macroscopic model……11

1-2.2. Microscopic model……14

1-2.3. Ion association in polymer electrolyte……16

1-3. Ionic transport properties……17

1-3.1. Conducting ion concentration……17

1-3.2. Conducting ion mobility……18

1-4. Purpose of this study……19

Chapter 2 Measurement of Conducting Ion Mobility and Concentration in Ion-containing Polymer using Dielectric Relaxation Spectroscopy……20

2-1. Plasticizing polyester ionomers with crown ether……20

2-2. Experimental……23

2-2.1. Materials……23

2-2.2. ^{1}H NMR……24

2-2.3. Dielectric relaxation spectroscopy……24

2-3. Results and discussion……25

2-3.1. ^{1}H NMR spectra……25

2-3.2. Dielectric spectra……27

2-3.3. Static dielectric constant……30

2-3.4. Ionic conductivity……32

2-3.5. Electrode polarization model……35

2-3.5.1. Conducting ion mobility……37

2-3.5.2. Conducting ion concentration……39

2-4. Summary……41

2-5. Future work……42

Chapter 3 Double a.c. Hall Effect Measurement of the Number Density of Charge Carriers and their Mobility……43

3-1. d.c. Hall Effect……43

3-1.1. Basic equations for d.c. Hall Effect……43

3-1.2. Measurement Procedures……47

3-1.3. Limitation of d.c. Hall Effect for Ionic Hall Effect ……50

3-2. a.c. Hall Effect……51

3-3. Results and discussion……54

3-4. Summary……60

3-5. Future work……61

Reference ……64

LIST OF FIGURES

Figure **1.1.** Ionic conductivity as a function of inverse temperature for various solid polymer electrolytes. 1, first-generation PEO-$LiCF_3SO_3$; 2, new solutes with high-dissociation PEO-$Li((CF_3SO_2)_2N)$; 3, low-T_g combination polymer; 4, plasticized polymer electrolyte PEO-$Li(CF_3SO_2)_2N$ + 25% w/w PEG-dimethylether; 5, gel-type polymer (cross-linked PEO-dimethacrylate-$Li((CF_3SO_2)_2N)$-PC 70%); 6, gel electrolyte P(VDF-HFP)/EC/DMC-$LiPF_6$……..……..……3

Figure **1.2.** Ionic conductivity versus temperature for the different solid electrolyte classes. The polymer electrolyte is a complex of Li triflate (trifluoroethylene sulfonate) with a host polymer of amorphous poly(ethylene oxide). AgI and β-alumina represent the salt and ceramic classes of Table 1.2, respectively. The ionomer, PE600-0.5Li, will be discussed in chapter 2…….....6

Figure **1.3.** Conductivity-temperature behavior of $LiBF_4$ complexes of PEO and PPO…….....10

Figure **1.4.** Schematic representation of sequential potential fields for ion conducting (a) inorganic salt crystal and (b) polymer electorlyte……..……..……14

Figure **2.1.** Chemical structure of 12-crown 4-ether ($C_8H_{16}O_4$)…….....22

Figure **2.2.** Chemical structure of the polyester random copolymer ionomers PE600-xLi (x=0.5)……..24

Figure **2.3.** ^1H NMR spectra of (a) PE600-0.5Li/50%12C4, (b) PE600-0.5Li/30%12C4, and (c) PE600-0.5Li/0%12C4……..26

Figure **2.4.** Dielectric loss at298 K for the PE600-0.5Li/0%12C4 (▲), PE600-0.5Li/10%12C4 (■), and PE600-0.5Li/10%12C4 (●).....28

Figure **2.5.** Derivative spectra at 263 K for the PE600-0.5Li/0%12C4 (▲), PE600-0.5Li/10%12C4 (■), and PE600-0.5Li/10%12C4 (●).....29

Figure **2.6.** Static dielectric constant as a function of inverse temperature for pure PE600-0.5Li ionomers, two mixtures of ionomers and 12-crown-4,and pure 12-crown-4……...30

Figure **2.7.** (a) Temperature dependence of ionic conductivity for PE600-0.5Li with 12C4 and without 12C4 (Lines indicate fits of the VFT equation (Eq. (2.2)) to the data) and (b) ac conductivity as a function of frequency at the several temperatures for PE600-0.5Li……..33

Figure **2.8.** Dielectric constant and loss as a function of angular frequency at 298 K for PE600-0.6Li. Lines are fits of Eq. (2.6) (dash line) and Eq. (2.9) (solid line) with n=0.884 to the data….....……..…..36

Figure **2.9.** Ion mobility vs inverse temperature. Lines are fits of Eq. (2.10) to the data....……...38

Figure **2.10.** Conducting ion concentration as a function of inverse temperature. Lines are fits of Eq. (2.11) to the data…….....……...39

Figure **3.1.** Schematic illustrating the Hall Effect in a p-type smaple…….…..…..45

Figure **3.2.** Different signs of charge carriers give different signs of Hall voltage …….……..46

Figure **3.3.** (a) Bridge-type Hall configuration, (b) and (c) lamella-type Hall configuration ……..48

Figure **3.4.** Chemical structure of the polyester copolymer ionomer PE600-xNa (x=10%)……...54

Figure **3.5.** Hall sample cell: (a) top view with a glass substrate and four Pt electrodes (b) cross section along cut A-A`…….……..55

Figure **3.6.** Four kinds of sample cells: (a) and (b) Cu electrodes, (c) and (d) Pt electrodes…….56

Figure **3.7.** Schematic illustrating the Hall sample holder with four-point probe……..57

Figure **3.8.** Measuring resistivity (a) and Hall coefficient (b) using a van der Pauw geometry……...……58

Figure **3.9.** Measured voltage: (a) $V_m(+)$ along + direction of magnetic field, (b) $V_m(-)$ along – direction of magnetic field…….....……59

Figure **3.10.** Voltage between the Hall contacts V_H recorded as a function of time for PEO-10%Na at $I = 0.3mA$, $B = 0.5T$, and $T = 298K$ ……....……..60

Figure **3.11.** Block Diagram for double a.c. Hall Effect measurements……..……...63

LIST OF TABLES

Table **1.1.** Modes of conduction in polymers……..…….....4

Table **1.2.** A classification of solid electrolytes…….……..…….....5

Table **2.1.** Integrated intensity of the α and β protons and actual wt % of crown ether…….....27

Table **2.2.** Parameters of the VFT equations for the DC conductivity and ion mobility....…….....34

Table **2.3.** Fitting parameters for Eq. (2.11) for the conducting ion concentration……....……...40

ACKNOWLEDGEMENTS

I would like to thank:

- My advisor, Professor Ralph H. Colby, for his advice and support throughout this thesis. He also showed me the way to be a good materials scientist via his outstanding knowledge and enthusiasm for research.

- The committee members of my thesis, Professor James Runt and Qiming Zhang, for their careful reading of my thesis.

- My group members, especially Wenjuan Liu, for her discussions about ion interactions and basically all the other subjects.

- All my good friends in MATSE department, especially Youmi Jeong, who has helped me greatly improve my understanding of the chemical aspects of my work. Dr. David J. Meyer for his help in the Hall Effect measurements.

- My father, mother, and sister, who always encouraged and support me to finish this work.

- My wife, Seung Kung, for everything else. This thesis could not be finished without her support and love.

Chapter 1

Introduction and Motivation

During the past two decades, the demand for the storage of electrical energy has grown rapidly, not only for portable applications such as cell phones and computers, but also for electric vehicles and for the effective commercialization of renewable resources such as solar and wind power.[1] Batteries are the systems with tremendous potential for such requirement, offering high energy density, flexible and lightweight design, and longer lifespan than comparable energy storage technologies.[2] A battery is composed of two electrodes connected by an ionically conductive material called an electrolyte, which enables ion transfer between the two electrodes. Battery performance involves complex, interrelated physical and chemical processes between electrode materials and electrolytes. Rechargeable, also known as secondary, batteries have developed over the years from lead-acid through nickel-cadmium and nickel-metal hydride (NiMH) to lithium-ion.[3] NiMH batteries were the initial workhorse for electronic devices, but they have almost been completely displaced from the market by lithium-ion because the lithium, with the highest oxidation potential of any element and low density, is in principle ideally suited for high energy density and design flexibility.[4]

Existing battery technologies have serious issues with: (1) cost, (2) limitation of energy storage capacity of individual battery cells, (3) the lack of fast recharge cycles with long cell lifetimes, and (4) safety. There has still been a significant lack of understanding of the mechanisms and kinetics of the elementary steps such as charge transfer phenomena and charge

carrier and mass transport that occur during battery operation even though batteries have been studied for 100 years. These insufficient technologies can bring us serious problems in terms of safety. For instance, highly reactive lithium metal in contact with a liquid electrolyte is dangerous because a lithium-metal/liquid electrolyte combination raises the growth of dendrites during each subsequent discharge-recharge cycle.[5,6] This potentially leads to not only explosion hazards but also reduced cycle lifetime. To circumvent the safety issues surrounding the use of the Li metal, the replacement of the liquid electrolyte with a solid polymer electrolyte (SPE) would be highly desirable.[7]

The first SPE showed a remarkably high degree of conductivity in alkali metal salts in polyethylene oxide (PEO).[8] The conductivity was 1×10^{-7} S/cm at room temperature. Alkali metal salts can be dissolved in PEO up to a maximum molar ratio of one of the salt to every four ether monomer unit. Typical salts are $LiClO_4$ and NaCNS. The presence of the lone pair of electrons on the oxygen atoms of the polyether allows a good solvating power to the well-know formation of crown ether complexes by certain cyclic oligomers of ethylene oxide.[4] The SPE also has features such as flexibility, processability, ease of handing and relatively low impact on the environment that polymers inherently posses. Their combination of solid yet flexible properties and film-forming ability with ionic conductivity makes them ideally suited for the development of rechargeable lithium batteries. Nevertheless, the SPE still poses the challenge of how close its electrochemical properties can be made to those of a liquid electrolyte cell with typical room temperature conductivity of 0.1 S/cm. Therefore, various efforts have so far been made to improve the ionic conductivity of the SPE. Figure 1.1 shows the ionic conductivity of various types of SPE. The efforts aimed at enhancing the ionic conductivity of polymer electrolytes have been insufficient to allow operation at room temperature. Therefore, there must be many fundamental performance characteristics required of polymer electrolytes to make them technologically viable. The issues of concern here include: conducting ion (1) conductivity, (2)

mobility, and (3) concentration. This thesis will concentrate on these, the more fundamental factors to better understand ion transport mechanism and how these are analytically characterized to achieve practical performance targets.

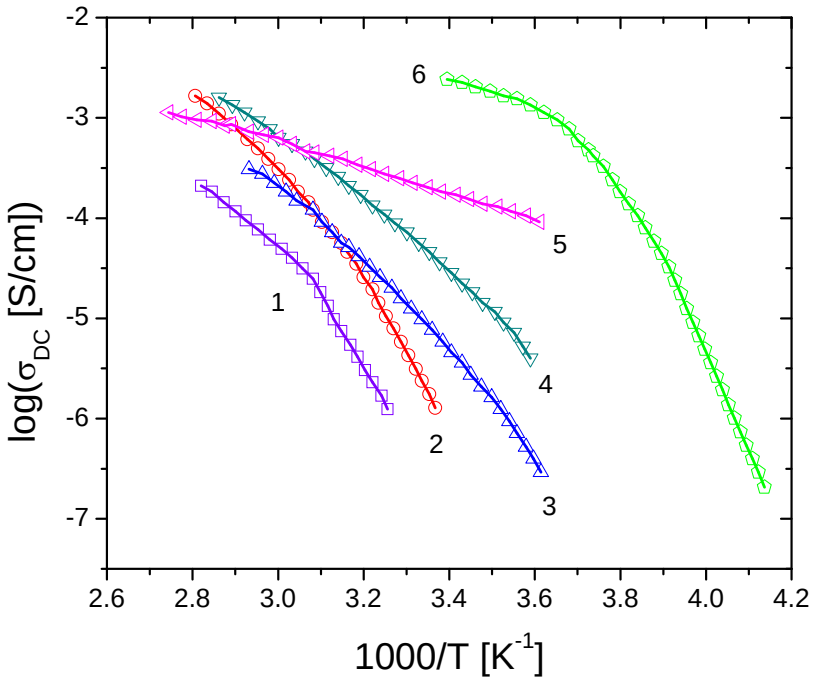

Figure 1.1. Ionic conductivity as a function of inverse temperature for various solid polymer electrolytes. 1, first-generation PEO-$LiCF_3SO_3$; 2, new solutes with high-dissociation PEO-$Li((CF_3SO_2)_2N)$; 3, low-T_g combination polymer; 4, plasticized polymer electrolyte PEO-$Li(CF_3SO_2)_2N$ + 25% w/w PEG-dimethylether; 5, gel-type polymer (cross-linked PEO-dimethacrylate-$Li((CF_3SO_2)_2N)$-PC 70%); 6, gel electrolyte P(VDF-HFP)/EC/DMC-$LiPF_6$.[2]

1-1. Historical development of polymer electrolytes for ion transport

In polymers, the total conductivity results from both electrons and ions. In a given case, however, it is likely that one type of conductivity will predominate. As illustrated in Table 1.1, conduction of polymers can be divided into electronic and ionic conduction modes. For electronic conduction, either electrons or holes may be the majority carrier and the process may be either intrinsic, a property of pure material, or extrinsic, a property of doped materials to obtain higher conductivity. Similarly, although the detailed mechanisms are quite different, ionic conductivity depends on the dissociation of pairs of positive ions (cations) and negative ions (anions). Thus, ionic conduction is provided by a strong correlation between relative permittivity and conductivity, which is readily explained by the reduction of the Coulombic forces between ions in a high relative permittivity medium. In this study we will focus on fully understanding conductivity in polymer ionics, or solid polymer electrolyte, rather than electronic conduction.

Table 1.1. Modes of conduction in polymers.[9]

I. Electronic	II. Ionic
Conduction by electrons or holes	Conduction by small cations and/or anions
(a) Intrinsic	(a) Intrinsic (self dissociating)
(b) Extrinsic (donor or acceptor)	(b) Extrinsic (impurities or dopants)

Historically, a solid electrolyte was first discussed carefully by Faraday[10], who concentrated on salts such as silver sulfide and lead fluoride. In the 1970s, polymer electrolytes were first reported by Fenton, Parker and Wright[11] and have been extensively developed by

Armand[12]. They lead to a fascinating range of physical properties, including the ability to transport cations or anions, or both, rapidly through a solid medium.

Table 1.2. A classification of solid electrolytes[13]

	Ceramic	Salt	Polymer	Glass
Ion pathways	Static	Static	Dynamic	Static
Conductivity	Activated (Arrhenius)	Faraday transition	Bent (VFT)	Activated (Arrhenius)

The most distinguished thing about polymer electrolytes within the general category of solid electrolytes (see Table 1.2) is that they are soft disordered materials. Structurally, polymer and glassy materials are amorphous, exhibiting short-range structural order and they generally reveal a glass transition temperature. Ceramic and salt materials, on the other hand, are a crystalline ionic conductors which have conduction pathways between favored sites such as vacancies. That allows ions to move from one site to another. As displayed in Fig 1.2, the ceramic and glassy materials show simple Arrhenius forms for the conductivity, given by

$$\sigma = \sigma_0 \exp\left(-\frac{A}{T}\right) \tag{1.1}$$

In polymer electrolytes, on the contrary, the curve is bent and is best fitted to an expression of the form

$$\sigma = \sigma_0 \exp\left(-\frac{B}{T - T_0}\right) \tag{1.2}$$

with prefactor σ_0 and Vogel temperature T_0, related to the glass-transition temperature T_g roughly by[14]

$$T_0 \cong T_g - 50\,\mathrm{K} \tag{1.3}$$

This is normally called VFT (Vogel-Fulcher-Tammann) behavior. The simplest understanding of VFT conductivity behavior is that conduction can occur only when the conducting ions move from one free volume space to another. The free volume model will be presented in Sec. 1-2.1 in detail.

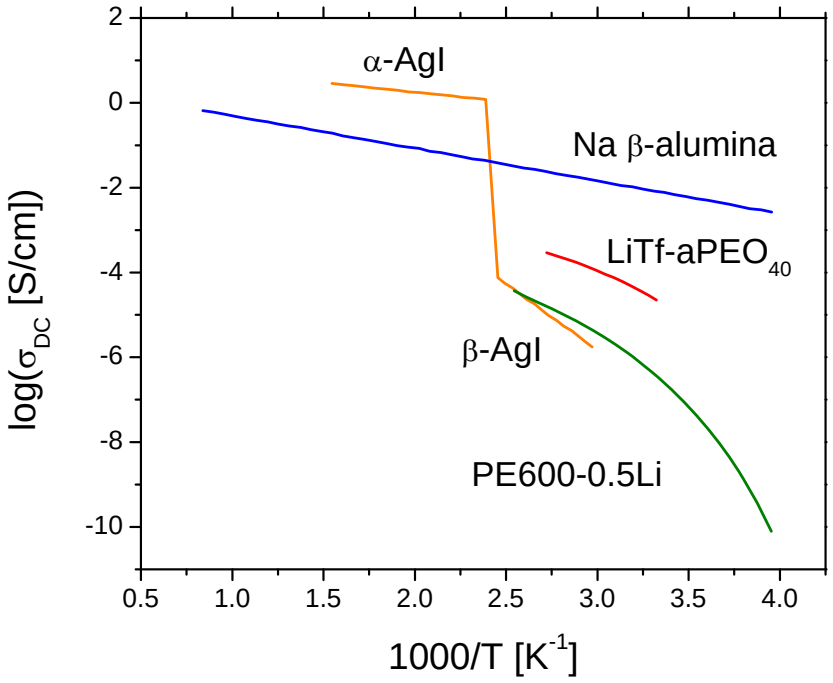

Figure 1.2. Ionic conductivity versus temperature for the different solid electrolyte classes. The polymer electrolyte is a complex of Li triflate (trifluoroethylene sulfonate) with a host polymer of amorphous poly(ethylene oxide). AgI and β-alumina represent the salt and ceramic classes of Table 1.2, respectively.[13] The ionomer, PE600-0.5Li, will be discussed in chapter 2.

For successful practical applications, a polymer electrolyte must have a range of critical properties including the following[15]: (1) adequate ionic conductivity, (2) high cation mobility with a unit transference number ($t_+ = 1$), (3) good mechanical properties, (4) the ability to form good interfacial contacts with electrodes, (5) a large electrochemical stability window, (6) ease of processing, (7) chemical and thermal stability, and (8) safety. Therefore, a number of new forms of polymer electrolyte have been developed to achieve the required performance[16]: (1) a plasticized electrolyte, usually obtained by the addition of small amounts of a high dielectric constant liquid to a solvating polymer electrolyte in order to enhance its conductivity, (2) a polymer-salt complex, consisting of a co-ordinating polymer, typically a polyether, in which a suitable salt co-crystallizes, (3) a single ion conductor, which has anions covalently bound to the polymer chain and hence only cations contribute to ionic conduction.

1-1.1. Plasticized polymer electrolyte

In order to further enhance ionic conductivity, plasticized systems in which the small molecule additive as a lubricant or the conducting phase itself have been studied. For lithium secondary batteries, Tsunemi et al.[17] used inorganic salts having low dissociation energy ($LiClO_4$) and organic solvents having both high boiling points and high room temperature dielectric constants (ε), such as propylene carbonate ($\varepsilon = 64.4$) and ethylene carbonate ($\varepsilon = 89.0$). These electrolytes were incorporated into such polymers having moderately high dielectric constant as polyvinylidene fluoride ($\varepsilon = 9.2$) and polyacrylonitrile ($\varepsilon = 8.0$). Ionic conductivity of 10^{-6} S/cm were observed in those systems at room temperature. Using a plasticizing solvent in a polymer-salt system is a fascinating option for enhancing the conduction properties. Plasticizers modify the electrolyte through an increase in configurational entropy, which consequently lowers

the T_g and increases ionic mobility.[16] Conductivity is critically affected by the physical properties of the solvent, which are viscosity, mobility, dielectric constant and ion solvation. A high dielectric constant increases the level of salt dissociation, while low viscosities lead to high ionic mobility. The main role of small molecules is therefore not only to plasticize the host polymer, improving flexibility and segmental motion, but also to solvate the cation which reduces ion-ion interaction energy.

1-1.2. Poly(ethylene oxide)-based polymer electrolyte

The development of ion-conductive polymers without organic solvent commenced with earnest in the 1980s after the reports of Wright and Armand. The study of PEO-salt complexes started from the analysis of the complex crystalline structures. The polymer-salt systems may be amorphous, crystalline or amorphous-crystalline mixtures, depending on the polymer, salt and preparation condition.[18] One model considered that a helical PEO chain surrounds cations to provide a specific path-way for cation transport.[19] Berthier et al.[20] reported that such crystalline phases are basically electrical insulators so that ion transport occurs principally in amorphous regions. However, the Bruce group[21-23] recently showed new crystalline polymer electrolytes with the 6:1 complex (PEO_6:$LiAsF_6$), involving very short PEO chains, make a unique exception to the rule that only amorphous polymers conduct.

To enhance ionic conductivity of polymer-salt systems, it will be necessary to facilitate the dissociation of inorganic salts in polymer. The thermodynamics of complexation has been considered in detail by Bruce.[24] The following requisites must be considered: (1) smaller lattice energy of an inorganic salt, (2) larger ion solvation energy from the polymer, and (3) higher dielectric constant of the polymer. The lattice energy of the salt depends on the charge density of

ions. Highly charged ions with small radii will lead to large lattice energies. In the case of polymer electrolyte, cations and anions are embedded in the polymer matrix; however, the anions are barely coordinated by the polymer chains. They are stabilized in the polymer electrolyte mainly by their attraction to the cations. In contrast, the cations are strongly coordinated by the ether-oxygen of the polymer host. The solvation of cations is determined by the donor number of the polymer and of anions by the acceptor number. A polyether such as PEO has a small acceptor number and high donor number, meaning that the ether-oxygen solvates the cation but not the anion.[25] The dielectric constant of a polymer matrix has an influence on the dissociation energy of inorganic salt. Barker[9,26] found that the logarithm of the ionic conductivity of many conventional polymers was proportional to the inverse of the dielectric constant ε of the polymer. In this case, the number density of ionic carrier, n, is expressed by

$$n = n_0 \exp\left(-\frac{W}{2\varepsilon kT}\right) \tag{1.4}$$

where n_0 and W are the total number density of ions and the dissociation energy of the salt, respectively. The dielectric constant of PEO, where the crystalline and amorphous phases coexist, is $\varepsilon = 4$ at 25 ^{0}C, while that of the amorphous phase is $\varepsilon = 8$.[27] This relatively high dielectric constant of amorphous PEO in comparison with those of typical polymers ($2 < \varepsilon < 10$) makes PEO more effective than most as a polymer matrix from the view point of salt dissociation. On the other hand, poly(propylene oxide) (PPO), which is fully amorphous, has a lower room temperature dielectric constant ($\varepsilon = 5.5$)[28], resulting in lower salt dissociation and ionic conductivity, shown in Fig. 1.3. However, the dielectric constant of PEO is considerably low in comparison with polar organic solvents such as propylene carbonate, $\varepsilon = 64.4$ at 25 ^{0}C.[16] The low dielectric medium makes it possible to form ionic clusters.[29] This ion aggregation can become a serious restriction for ionic conductivity.

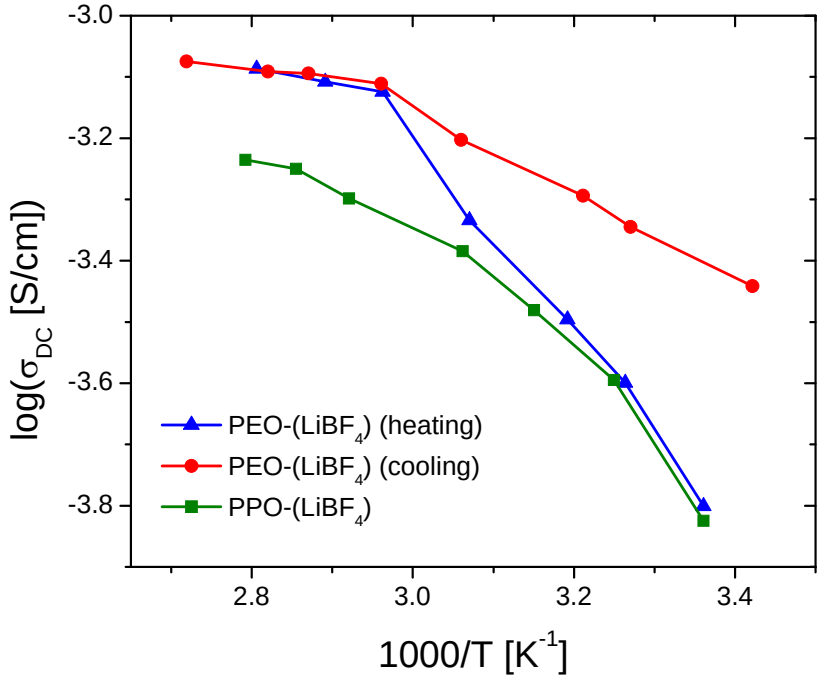

Figure 1.3. Conductivity-temperature behavior of $LiBF_4$ complexes of PEO and PPO.[30]

1-1.3. Single ion conductors

In the ordinary solid polymer electrolytes with dissolved salt, a significant decrease in ionic conductivity occurs under direct current during discharge.[31] This is due to the fact that there is no electrode reaction for the anions, which move faster than the cations and accumulate at the anode unless the salt diffusion coefficient is sufficiently large to allow the concentration gradient to relax.[32] This accumulation of anions lowers the field that moves the cations, resulting in voltage losses owing to concentration polarization that may cause poorer performance and even

undesirable change in the electrolyte state such due to phase transitions and salt precipitation.[33] There is therefore an essential requirement that the SPE is designed to have only cation migration. Such materials are called single ion conductors. In addition, the single ion conductors are expected to attain larger energy densities and high power densities.[34]

To avoid concentration polarization, the free movement of anions needs to be either limited or totally eliminated. The former case is related to the simple introduction of anion trapping sites to polymer electrolytes, to retard the free movement of anions. Mehta et al.[35-37] individually examined the boron-in-chain type solvent-free polymer electrolyte. Their boroxine ring containing polymer electrolyte showed high t_{Li^+} of 0.7. The Angell[38-40] group also reported anion-trapping and polyanion electrolytes based on acid-in-chain borate polymers to improve the cation transference number. The ionic conductivities reached 7.6×10^{-5} S/cm at 25 ^{0}C. The latter case arises from covalently bonding anions to the polymer backbones to form single ion conductors with a unity lithium transference number. Different strategies have been used in the synthesis of single ion conductors. Anions have been incorporated into side chains of comb-branched polymer[33,41,42], have been mixed with polyether electrolytes[43], and have been attached to the linear poly(ethylene glycol) (PEG) chain.[44-47] In this thesis we will fully explore ion transport mechanisms of single ion conductors.

1-2. Ion-conduction mechanisms in polymers

1-2.1. Macroscopic model

Ionic transport in single-ion conductors differs from that in conventional liquid electrolytes or polymers with dissolved salts. In the latter systems, ions might be imagined to

move with their co-ordination spheres but in the case of high molar mass polymers, this cannot happen. The polymer chains cannot move significant distances and it is necessary for ions to dissociate to some extent from their co-ordination sphere in order to move through the polymer matrix. Consequently, a different ion transport mechanism must operate. Extensive work has been done in modeling and understanding transport mechanisms in polymer electrolytes.[48] Miyanmoto and Shibayama[49] derived the ionic conduction in polymers based on a free-volume theory:

$$\sigma = \sigma_0 \exp\left[-\left\{\gamma V_i^* / V_f + \left(E_j + W/2\varepsilon\right)/kT\right\}\right] \tag{1.5}$$

where E_j is the activation energy for ion transfer in polymer, W is the dissociation energy of a salt in polymer, ε is the dielectric constant of polymer, k is Boltzmann's constant, T is the absolute temperature, γ is a numerical factor to correct for the overlap of the free volume, V_i^* is the minimum hole size necessary for ion transfer, formed by thermal fluctuation of the free volume, and V_f is the average free volume per ion above a glass transition temperature ($T > T_g$), given by

$$V_f = V_g\left[f_g + \alpha\left(T - T_g\right)\right] \tag{1.6}$$

where V_g, f_g and α are the relative volume at T_g, the free-volume fraction at T_g, thermal expansion coefficient of the free volume, respectively. From Eq. (1.5) and (1.6) a system which has a high dielectric constant and a sufficient free volume (far above T_g) can show relatively high ionic conductivity. Williams, Landel, and Ferry[14,50] introduced the WLF equation which describes the temperature dependence of dielectric or mechanical relaxation times for the local main-chain motion of many amorphous polymers:

$$\log\frac{\sigma(T)}{\sigma(T_g)} = \frac{C_1\left(T - T_g\right)}{C_2 + \left(T - T_g\right)} \tag{1.7}$$

where C_1 and C_2 are the WLF parameters of the free-volume equation for the ionic transport.

The WLF equation itself is an empirical equation, rather than the result of any theoretical approach. In an attempt to understand how the conductivity mechanism works, quasi-thermodynamic theories which were developed by Cohen and Turnbull[51] (free volume theory) and by Adam and Gibbs[52] (configurational entropy theory) have been applied with some success to consideration of transport properties in polymer electrolytes. These theories indicated that above T_g, the polymeric material becomes macroscopically rubbery rather glassy, in other words, any given polymer chain becomes locally mobile at the glass transition. Therefore, it is only the thermal energy in excess of the glass transition temperature that provides actual mobility of the local polymer chain segments.[51,52] In this sense, one is not surprised that the Arrhenius behavior, involving inverse temperature, is replaced by the VFT involving the inverse of $T - T_0$. The fact that the temperature dependence of the ionic conductivity follows the WLF equation means that ion conduction in polymer solids significantly relies on the segmental motion of polymer chain: that is, the dissociated cation which is stabilized by the coordination of more than one ether oxygen is coupled with the segmental motion as well.[25]

To understand this mechanism from the point of view of potential fields, the ion transport mechanism of the inorganic salt crystals is compared with that in polymer electrolyte (see Fig. 1.4). In the inorganic salt, a potential-energy barrier is generated by the crystal field, and the ion migration is due to a ion hopping mechanism whereby ions hop over the barrier.[53] Even if it seems difficult to migrate ions in polymer solids, segmental motion makes it possible for ions to migrate in the matrix. Thus, higher segmental motion at room temperature is required to lower the effective barrier and produce good ion conduction.

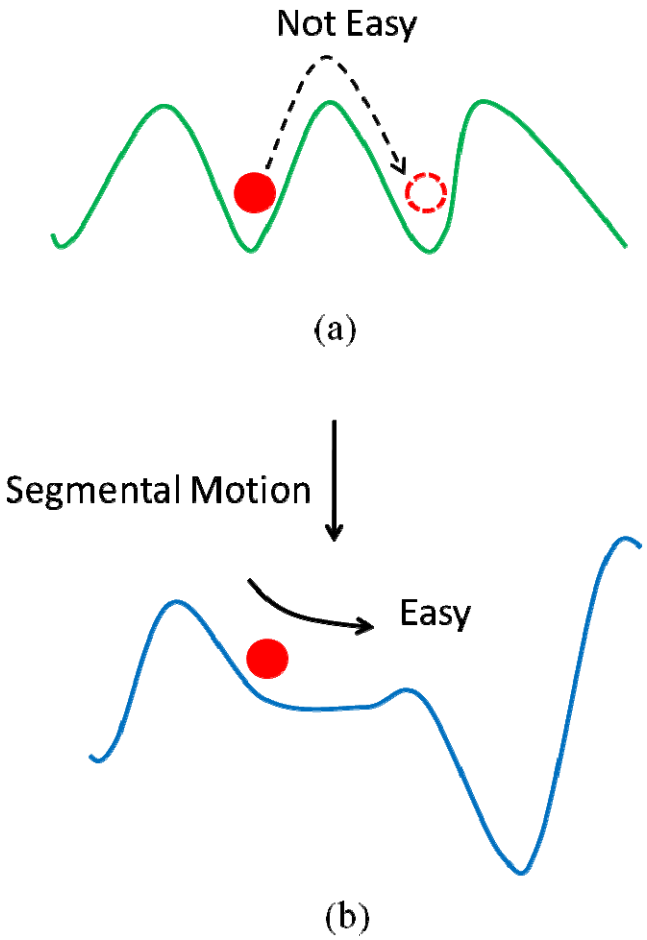

Figure 1.4. Schematic representation of sequential potential fields for ion conduction (a) inorganic salt crystal and (b) polymer electrolyte.[25]

1-2.2. Microscopic model

While quasi-thermodynamic approaches such as free volume and configurational entropy models give impressive qualitative understandings of conductivity in polymer electrolytes, a more microscopic model, which describes the actual motion of individual ions, is of great value in correlating designable properties such as ionic charge, charge density, polymer flexibility, and

interactions with transport.[13] Such a model is the dynamic bond percolation (DBP)[54-59] model , which was originally developed to deal with polymer/salt complexes. The model is intended to describe diffusion of ions in a disordered medium undergoing dynamic rearrangement processes on a timescale short compared to the observation time. The model is characterized by three factors: an average hopping rate between two sites available for ionic occupancy w, a relative probability of a given site being available f , and a mean renewal time $\bar{\tau}_{ren}$ for dynamic motion of the medium to rearrange the assignments of closed and open bonds.[55] In the standard percolation model, the hopping is either permitted or not permitted[55]:

$$w_{ij} = \begin{cases} 0, & \text{probability } 1\text{-}f \\ w, & \text{probability } f \end{cases} \tag{1.8}$$

Each hopping rate is defined as either 0 (the hopping is forbidden) or w (the hopping is allowed). Their relative probabilities are given by f and $1-f$, respectively. Then, in the simplest one-dimensional model, the diffusion coefficient obeys[55]:

$$D \sim \left\langle X^2 \right\rangle_0 / \bar{\tau}_{ren} \tag{1.9}$$

Here the numerator is the mean-square displacement of the ion in the absence of renewal, and the denominator is the average renewal time. This time corresponds to a characteristic relaxation time for a polymer's configurational degree of freedom. Equation (1.9) indicates that the diffusion coefficient is inversely proportional to the renewal time, which, in turn, is proportional to segmental relaxation time of the polymer host. Therefore, the DBP model explains the coupling between ion transport and polymer relaxation.

1-2.3. Ion association in polymer electrolyte

Liquid electrolyte solutions are sufficiently dilute (1-10 millimolar) to be described by the Debye-Huckel[60] or Onsager[61,62] models. Their theories suggested that there is a tendency for ions having a charge opposite to that of the central ion to be sufficiently dispersed around the central ion so that the diluted system forms an ionic atmosphere around a central ion. By contrast, molten salts are very concentrated (typically 20 molar), ion-ion interactions are pronounced, and alternative theories such as that of Fuoss[63] are required. Polymer electrolytes typically have (repeat unit):(cation) ratios, n, in the range 8 to 30, corresponding to 0.7 to 2.5 molar for PEO_n:$LiClO_4$[64] and ion aggregations such as ion pairs, triples, or quadrupoles are an important factor of their behavior.

Since the ion clusters can contribute to the conduction process, it is necessary to understand ion aggregation. In the medium of low dielectric constant, ions will tend to associate under the influence of coulombic forces to form ion pairs, triplets, and higher aggregates. The formation constants for the steps in this association can be expressed in terms of the degree of association, $(1-\alpha)$, which, in turn, can be expressed in terms of probability of the ions being a interionic distance apart, using the Maxwell-Boltzmann distribution law.[65] In 1926 Bjerrum first treated the ion pair formation with this method. Fuoss and Kraus[66] extended the dissociation constant in terms of the size of the ions involved and the dielectric constant of the solvent. They also introduced the dissociation constant of triple ions, formed from a neutral molecule and a simple ion by the action of electrostatic forces.[67] Pettit and Bruckenstein[29], furthermore, considered the formation of higher aggregates up to sexapoles. In spite of these pioneering works, it is difficult to define the structure of charge carriers (single ions, ion triples, etc.) in the conduction process of polymer electrolyte. This problem causes a wrong result which is that

many calculations only consider the model of single ions. It is important, therefore, to gain theoretical understanding of formation of ion complexes and to validate the theoretical findings with the suitable experimental methods.

1-3. Ionic transport properties

1-3.1. Conducting ion concentration

The ionic conductivity σ can be simply expressed by

$$\sigma = ne\mu \tag{1.10}$$

where n, e and μ are total number density of conducting ions, elementary electric charge, and conducting ion mobility, respectively. To design ion-conducting polymers with a high ionic conductivity, an effort must be made to increase the two factors n and μ. For a salt dissolved in a polymer host, the formation of ion pairs produces neutral species and the concentration of conducting ions decrease. Although larger aggregates such as triple ions may be charged, their mobilities will be compensated by size in comparison to free ions and the conductivity will be reduced again. For these reasons, it is necessary to understand ion association and measure the number density of each state when considering ion transport in polymer electrolytes. MacCallum et al.[68] obtained the dissociation constant of pair and triplet ions through the conductance measurement and calculated the concentration of ions in each state. Torell and Schantz et al.[69-72] developed the analyses of the ion aggregation phenomena in PPO and PEO based $NaCF_3SO_3$, $LiCF_3SO_3$, and $LiClO_4$ complexes as functions of salt concentration and temperature by using Raman spectroscopy. They showed that the amount of dissociated ions, n, decreases as temperature is raised in an Arrhenius fashion. This result, however, is different from that

indicated in Eq. (1.4), which is that the number of dissociated ions is considered to increase as temperature is raised. The reason is that Torell and Schantz used Raman spectroscopy to measure an increase in the contact pair population as temperature is raised, from which they infer that the free ion content decreases. In the case of separated pairs, on the other hand, the perturbation of the vibrational states of the anion is usually too small to be detected.[46] Thus, both separated pairs and unpaired ions are spectroscopically counted as being free.

1-3.2. Conducting ion mobility

The mobility of conducting ions is obviously a crucial factor in terms of fast and/or deep discharge, energy density, and cycle number. As with the identification of specific charged species in polymer electrolytes, the relative mobilities of these species and the actual measurement of their relative mobilities remain among the most controversial issues yet to be resolved. There are numerous techniques available for measuring transport properties: Tubandt-Hittorf methods[73,74], radiotracer diffusion measurements[75], and pulsed field gradient (PFG) NMR diffusion measurement[76,77]. The Tubandt-Hittof method is to detect the net response only of charged species when an electrolyte is polarized. Its disadvantage is that low currents must be employed to prevent the use of large potential differences which might promote the degradation of the polymer at the electrode/electrolyte interface.[74] Diffusion techniques such as PFG NMR are purely nuclei sensitive and do not respond to the electric field. As a result, the combined flux of both charged and electrically neutral species such as ion pairs is measured.

1-4. Purpose of this study

Although both Raman spectroscopy and NMR allow the determination of ion mobility and ion association, the measured results are still unsatisfactory and not fully understood. These relate particularly to the inadequate understanding of the mechanism of ion transport. Thus, the two most important factors of ion transport to optimize the design of polymer electrolyte must be addressed: (1) ion mobility and (2) conducting ion concentration. In chapters 2 and 3 we present the relationship between these two factors in single ion conductor systems using two very different methods. We believe that our work provides a promising approach to understand the mechanism of ion transport in polymer systems and hope that this will be useful to allow a design of high energy density, high power density, and safe rechargeable batteries.

Chapter 2

Measurement of Conducting Ion Mobility and Concentration in Ion-containing Polymer using Dielectric Relaxation Spectroscopy

Ionic conduction in ion-containing polymers is of considerable interest from both fundamental and applied viewpoints. Recently, scientists are attempting to understand ion-containing polymers for advanced devices such as electrochemical membranes for lithium batteries and fuel cells and electromechanical devices for actuators and sensors. From the fundamental side, we do not yet understand how to design ion-containing polymers to have a large and rapid flux of ions in response to an applied field. Therefore, precise measurements of number density and mobility of charge carriers is vital to optimize the design of ion-containing polymers as well as better understand the generation and transport processes of ionic carriers in these polymers. Ionic conductivity in ion-containing polymers can be measured by using dielectric relaxation spectroscopy. A physical model of electrode polarization makes it possible to determine ionic mobility and conducting ion concentration as a function of temperature as well.

2-1. Plasticizing polyester ionomers with crown ether

We design, synthesize and characterize poly(ethylene oxide) (PEO) based polyester copolymer ionomers that have anions bound to the polymer chain, with Li^+ counterions. These

soft ionomers are single-ion conductors that are potentially useful as separators between the electrodes of a lithium battery[47]. Lightly sulfonated ionomers that are primarily PEO exhibit room temperature conductivities that are too low to be practical[47,78]. Analysis of electrode polarization in dielectric spectroscopy reveals the reason for this low conductivity: only a tiny fraction of Li^+ counterions are participating in conduction[47], owing to the strong interaction between sulfonate and Li^+ in the low dielectric constant medium of PEO. Various approaches have been adopted in order to improve the ionic conductivity of polymer electrolyte systems. These include: (1) modification of the PEO host[79], (2) customized design of a variety of host polymers[80], and (3) the use of additives such as plasticizers.[81] The focus of the present study is the effect of the addition of crown ethers on the conductivity of PEO-based polymer electrolytes.

The discovery of the crown ethers by Pedersen[82] stemmed from efforts to control the catalytic activity of vanadium and copper by complexation with multidentate ligands. The first identified crown ether, named dibenzo-18-crown-6, was not the target of synthesis in his experiment but a slight amount of unexpected by-product in a 0.4 % yield. However, his appreciation of the importance of the discovery, followed by energetic research in the area, established the foundation for the present status of crown ethers throughout the world. The most striking characteristic of crown ethers is their selective complexation ability. They bind the cationic portion of alkali and alkaline earth metal salts, ammonium salts and ionic or polar organic compounds (guest), into the cavity of the crown ring (host).[83] The complex of crown ether with a guest is formed by ion-dipole interaction between the cation and the lone pairs of electrons in the oxygen atoms in the ring structure of the cyclic polyether. The selectivity of crown ether for a given cation is dependent principally on the following points: (1) relative size of the cavity of the crown ring and the diameter of the cation, (2) number of donor atoms in the crown ring and the topological effect, (3) the relationship between the hardness of the cation and that of the donor atom, and (4) valence of the cation.[84] Therefore, much interest has been focused

to the effects of crown ethers on the electrochemical properties of solid electrolyte systems. Some of the earliest work using crown ether in polymer-salt complexes was that of Kaplan et al. who observed the effect of the addition of crown ether to poly(vinylene carbonate) containing lithium trifluoromethanesulfonate ($LiCF_3SO_3$).[85,86] Nagasubramanian et al. showed that the addition of 12-crown 4-ether (12C4) to PEO electrolytes containing $LiCF_3SO_3$, $LiBF_4$, or $LiClO_4$ improved the ionic conductivity of PEO electrolytes.[87,88] Matsuda group investigated the effects of 12C4 or 15C4 on the conducting behavior of complexes of PEO-grafted poly(methylmethacrylate) (PEO-PMMA) and lithium (Li) salts. The addition of crown ethers improved the ionic conductivity.[89] The crown ethers are macrocylic compounds in which ether oxygens inside of the ring structures are perfectly arranged to permit metal ions to enter and interact with the oxygen lone pairs.[90,91] incorporation of crown ethers may lead to fast cationic conduction in ion-containing polymers owing to the hypothesis that the crown ethers may create a natural ion channel where a cation may be able to easily enter and move.[92]

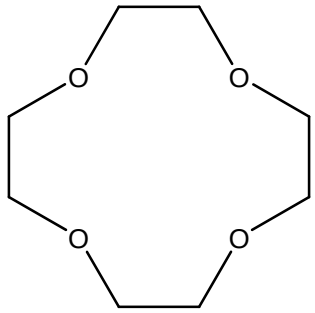

Figure 2.1. Chemical structure of 12-crown 4-ether ($C_8H_{16}O_4$)

In this chapter we describe an approach to improving the ionic conductivity of PEO-based ionomers which involves the incorporation 12C4 (see Fig. 2.1). The useful property of the 12C4 for its application is that Li^+ is surrounded by two separate 12C4 entities to form a puckered

sandwich arrangement, being coordinated only by the crown ether oxygens.[93] Thus, these structure types can demonstrate the use of crown ether in effecting cation and anion separation. In this study we add crown ethers to sulfonated ionomers that are PEO-based and measure conductivity by dielectric relaxation spectroscopy.

2-2. Experimental

2-2.1. Materials

Sodium polyester ionomers synthesized by Shichen Dou[47,94] were dissolved in water and then diafiltered with deionized water using an Amicon 1000 molecular weight cut-off membrane. Those ionomers were then dissolved in 0.5 *M* $LiCl/H_2O$ and diafiltered to exchange the sodium to lithium (Li^+). Diafiltration was considered complete when the dialyzate exhibited constant conductivity (~ 10 μS/cm). The concentrated ionomer solution was then freeze dried and vacuum dried at 120 ^{0}C to constant mass. The polymer is labeled PE600-xLi where x is the fraction of ionic isophthalate groups that are sulfonated. The structure of the ionomers is shown in Fig. 2.2. 1,4,7,10-Tetraoxacyclododecane (12-crown 4-Ether) (95+ %), supplied by Tokyo Chemical Industry, was added to a know mass of PE600-0.5Li ionomer in Teflon plate with a ratio of 12C4 to PE600-0.5Li of 0.3:1 and 0.5:1. The PE600-0.5Li ionomer without crown ether was also prepared for comparison of their ionic conductivity. These samples were stored inside desiccators for 50 days before measurement in order to provide enough time for 12C4 to fully diffuse into the ionomer. ^{1}H NMR was used to confirm the structure of the polymer as well as the 12C4 content.

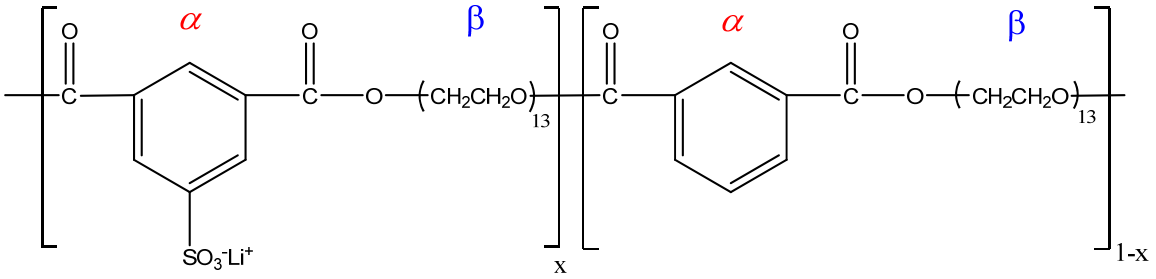

Figure 2.2. Chemical structure of the polyester random copolymer ionomers PE600-xLi (x=0.5).

2-2.2. ^{1}H NMR

^{1}H NMR spectra were recorded on a Bruker DPX-400 spectrometer with XWINNMR software. Typically 20 mg of samples were dissolved in 0.6 ml of a deuterium oxide solvent (D_2O, 99.9 %) which was supplied by Combridge Isotope Laboratories. The spectra were used to verify the ionomer structure and to quantitatively determine the amount of crown ether inside the ionomers. That will be discussed in Section. 2-3.1.

2-2.3. Dielectric relaxation spectroscopy

The ionomers with 12C4 are liquids at room temperature. A dry melt ionomer was transferred onto one brass electrode with 3 cm diameter. To control the sample thickness at 50 μm, silica spacers were placed on top of the sample after it had flowed to cover the electrode. The second electrode was placed on top and gravity formed a 50 μm sandwich as the extra sample was squeezed away. The sandwiched ionomers between two electrodes were placed in the

Novocontrol GmbH Concept 40 broadband dielectric spectrometer, after being dried in a vacuum oven for 24 h at 80 ^{0}C. The dielectric permittivity was measured using an AC voltage amplitude of 0.1 V for all experiments. Frequency sweeps were performed isothermally from 10 MHz to 0.01 Hz in the temperature range from -20 to 60 ^{0}C for the samples with crown ether or from -20 to 120 ^{0}C for the sample without crown ether because the boiling point of 12C4 is between 61 and 70 ^{0}C. The analyses of conductivity and electrode polarization are described in Secs. 2-3.4 and 2-3.5, respectively.

2-3. Results and discussion

2-3.1. ^{1}H NMR spectra

Figure 2.3 shows the ^{1}H NMR peak assignments for the PE600-0.5Li ionomers with and without crown ether. In the system with crown ether we can observe the chemical shift at ~3.6 ppm. On the other hand, the neat ionomer does not show such a peak at 3.6 ppm. Basically, the peak between 3.3 and 4.0 ppm is assigned to the NMR absorbance of ether groups.[95] The peak at ~3.6 ppm is assigned to the adsorption of crown ether. The three peaks at about 7.8, 8.3, and 8.6 ppm are assigned to the NMR absorbance of α aromatic protons. The chemical shifts between 3.4 and 4.5 ppm correspond to β protons. The ^{1}H NMR peaks of the protons in the repeat unit do not overlap with other peaks, the relative quantity of crown ether can be evaluated from the integrated intensity of the protons in the repeat unit (see Table 2.1). From the result, only a tiny fraction of crown ether is present, most was lost in the vacuum oven drying.

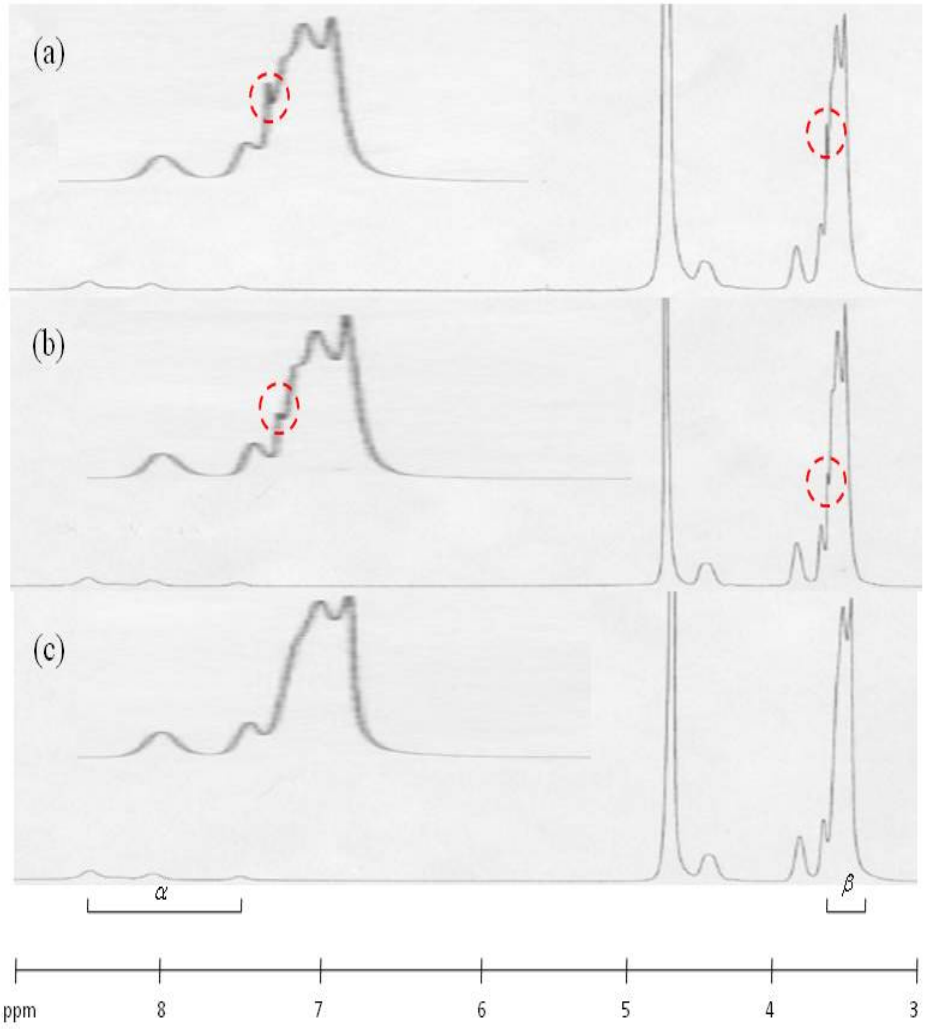

Figure 2.3. ^{1}H NMR spectra of (a) PE600-0.5Li/50%12C4, (b) PE600-0.5Li/30%12C4, and (c) PE600-0.5Li/0%12C4.

Table 2.1. Integrated intensity of the α and β protons and actual wt % of crown ether.

Sample	wt % of crown ether added	α	β	β/α	wt % of crown ether in sample
PE600-0.5Li/0%12C4	0%	7.06	91.42	12.95	0%
PE600-0.5Li/10%12C4	30%	7.77	110.57	14.23	10%
PE600-0.5Li/12%12C4	50%	7.48	108.64	14.52	12%

2-3.2. Dielectric spectra

To validate the expected hypothesis, we investigate not only the transport of Li^+ but also the local dynamics in these systems, using dielectric relaxation spectroscopy. Figure 2.4 shows dielectric loss $\varepsilon''(\omega)$ spectra for PE600-0.5Li/0%12C4, PE600-0.5Li/10%12C4, and PE600-0.5Li/12%12C4 at 298 K, well above their glass transition temperature T_g. In dielectric loss spectra, an electrode polarization (EP) peak is observed for these ionomers. The EP frequency for the ionomer with 12C4 ($\omega_{EP}^{12\%}$ or $\omega_{EP}^{10\%}$) is higher than that for the ionomer without 12C4 ($\omega_{EP}^{0\%}$). The crown ether clearly increases the conductivity, and also speeds electrode polarization. 12C4 may effectively gives rise to both cation solvation and anion separation due to the fact that lithium ions sit above the ring plane of 12C4[96], so that 12C4 makes it possible to provide more facile Li^+ mobility.

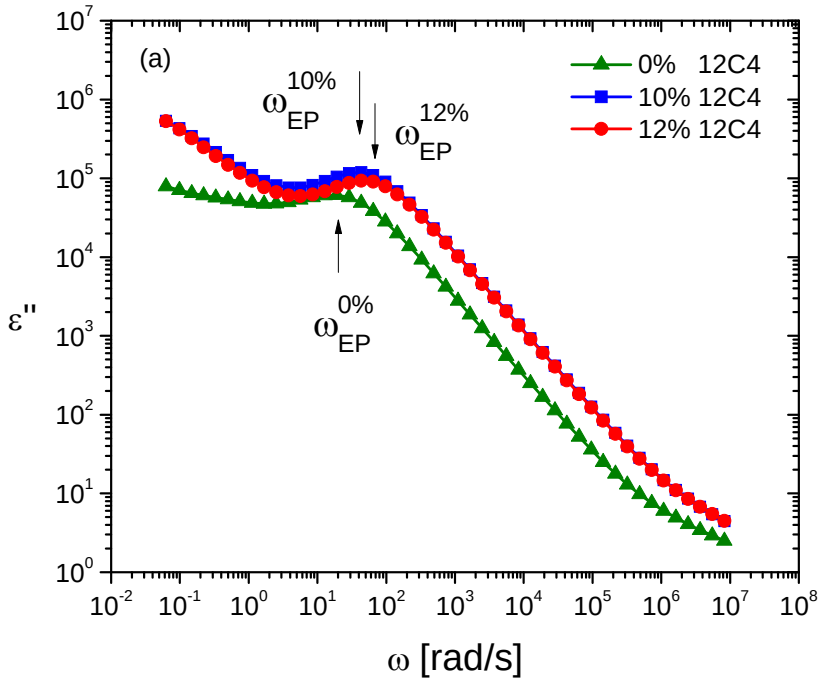

Figure 2.4. Dielectric loss at 298 K for the PE600-0.5Li/0%12C4 (▲), PE600-0.5Li/10%12C4 (■), and PE600-0.5Li/12%12C4 (●).

To assess how important the influence of crown ether is on the polymer relaxation, we need loss peaks to show dipolar relaxation processes. However, it is not clear to observe dielectric relaxation processes on the dielectric loss spectra of the ionomers since conduction and electrode polarization can mask the dielectric response of the sample.[97] Thus, we used the derivative formalism to understand the relaxation process in the temperature range[98] where EP and conductivity dominate;

$$\varepsilon_{der}(\omega) = -\frac{\pi}{2}\frac{\partial \varepsilon'(\omega)}{\partial \ln \omega} \qquad (2.1)$$

The results are presented in Fig. 2.5. A α process corresponding to the segmental relaxation of the polymer backbone is observed on the three systems. The frequencies of the α process are similar. This result indicates that the addition of crown ether in the ionomer has no influence on the segmental motion of polymer, but enables lithium ion to move from site to site aided by cooperative motion of crown ether.

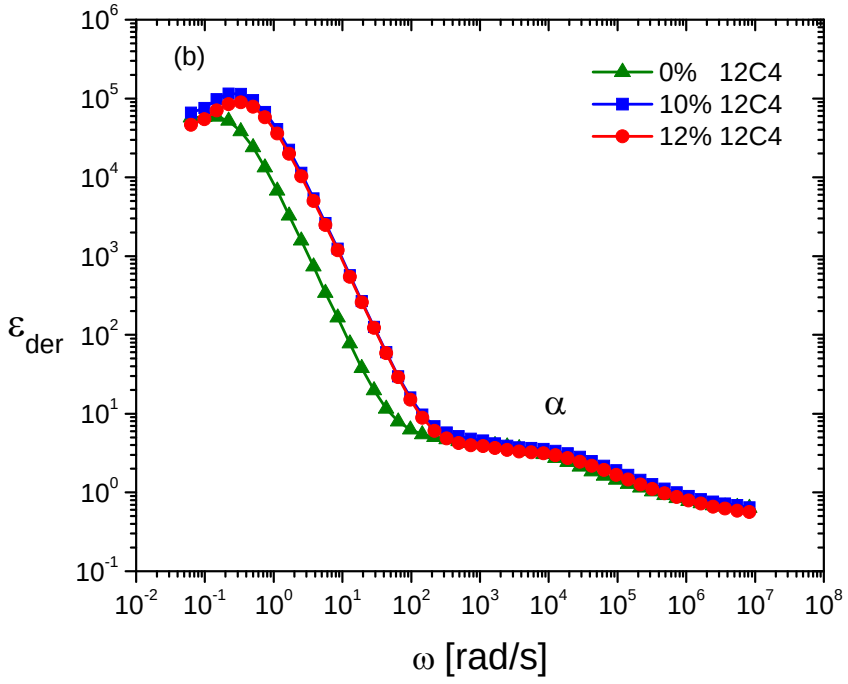

Figure 2.5. Derivative spectra at 263 K for the PE600-0.5Li/0%12C4 (▲), PE600-0.5Li/10%12C4 (■), and PE600-0.5Li/12%12C4 (●).

2-3.3. Static dielectric constant

The application of a steady electric field to a system of dipolar molecules results in a net orientation of the dipoles in line with the applied field. The most common polarity scale relies on the static dielectric constant ε_s which reflects the orientational polarization caused by molecular dipole moments and the molecular polarizability.[99] The value of ε_s, shown in Fig.2.6, was obtained from the low-frequency plateau of the $\varepsilon'(\omega)$ spectra after subtraction of EP.

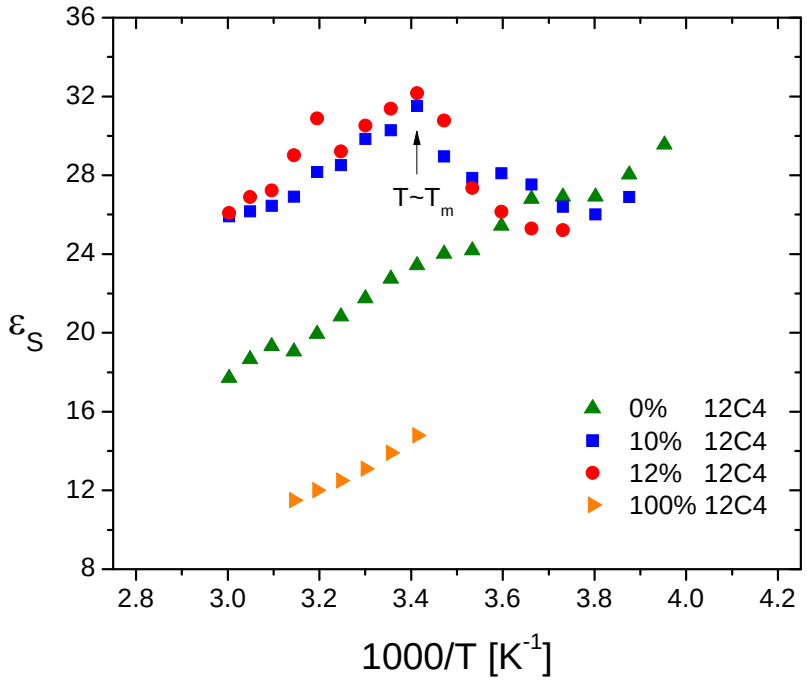

Figure 2.6. Static dielectric constant as a function of inverse temperature for pure PE600-0.5Li ionomers, two mixtures of ionomers and 12-crown-4, and pure 12-crown-4.

At lower temperature the dielectric constants for both ionomers with and without crown ether are close to each other. Near the melting temperature (T_m) of the crown ether or above T_m, however, the ε_s for the ionomer combined with crown ether is higher than that of the neat ionomer. Fragiadakis[46] concluded that PEO-based polyurethane ionomers with lithium, where its chemical structure is similar to this system, tend to form primarily ion pairs and quadrupoles, the latter having no dipole moment. The fact that crown ethers form stable complexes with lithium ions enables separating the quadrupoles into ion pairs. Presumably the crown ether can easily interact with Li^+ in the ion pair but not so easily with the quadrapole. That contributes to the increase of the static dielectric constant. The static dielectric constant of dipolar molecules can be also understood in terms of the Onsager equation[47,61]

$$\frac{(\varepsilon_s - \varepsilon_\infty)(2\varepsilon_s + \varepsilon_\infty)}{\varepsilon_s(\varepsilon_\infty + 2)^2} = \frac{Nm^2}{9\varepsilon_0 kT} \tag{2.2}$$

where N and m are the number density and dipole moment of the dipoles, respectively, ε_∞ is the high-frequency limit of the dielectric constant, ε_0 is the permittivity of vacuum, and k is Boltzmann's constant. The Onsager equation can be reduced to

$$\varepsilon_s = \frac{A}{2} + \sqrt{\frac{A^2}{4} - \frac{\varepsilon_\infty{}^2}{2}} \quad with \quad A = \frac{\varepsilon_\infty}{2} + \frac{Nm^2}{18\varepsilon_0 kT}(\varepsilon_\infty + 2)^2 \tag{2.3}$$

The simplified Onsager equation suggests that the system which has larger dipole moment of the dipoles makes it possible to show higher static dielectric constant. The dipole moment for a sulfonate-Li ion pair is $m_{pair} = 5.74$ D, obtained using *ab initio* calculation in vacuum. On the contrary, the values of m_{pair} for a crown ether-Li ion pair are 17.14 D in the same surrounding medium, assuming all ions are in ion pairs. The larger dipole moment for a crown ether-Li ion pair has a significant influence on effective dipole moment for a sulfonate-lithium ion pair in the ionomer with crown ether. For example, an average distance between cation and anion of the ion

pair would increase due to the complex of crown ether with Li^+. The larger distance, therefore, corresponds to a larger dipole moment than a just contact pair. The strong decrease in ε_s with increasing temperature due to thermal randomization is a consequence of the factor $1/T$ in the Onsager equation (thermal randomization of dipoles).

2-3.4. Ionic conductivity

Figure 2.7 describes d.c. conductivity of these ionomers as evaluated from a roughly 3-decade frequency range where the in-phase part of the conductivity $\sigma'(\omega) = \varepsilon''(\omega)\varepsilon_0\omega$ is independent of frequency. With increasing temperature, the dc conductivity increases rapidly. Interestingly, the ionic conductivity for PE600-0.5Li with crown ether is higher than that without crown ether. The addition of crown ether improves the ionic conductivity. It is generally observed that the addition or mixing of crown ethers to organic solutions of Li salts enhances the ionic conductivity.[100] The affinity of oxygen in the crown ether toward Li^+ encourages ionic dissociation of the salt in the solution. This would be the case for the ionomers with 12C4. The lithium ion dissociated from sulfonate anion owing to the selectivity of crown ether takes part in ion conduction. In order to investigate the mechanism of conduction in more detail, we fit the temperature dependence of conductivity to a Vogel-Fulcher-Tammann (VFT) equation:

$$\sigma_{DC} = \sigma_0 \exp\left(-\frac{BT_0}{T - T_0}\right) \tag{2.4}$$

where σ_0 is a constant, T_0 is the Vogel temperature where the free volume is zero, and B is the so-called strength parameter related to the divergence from Arrhenius temperature dependence.

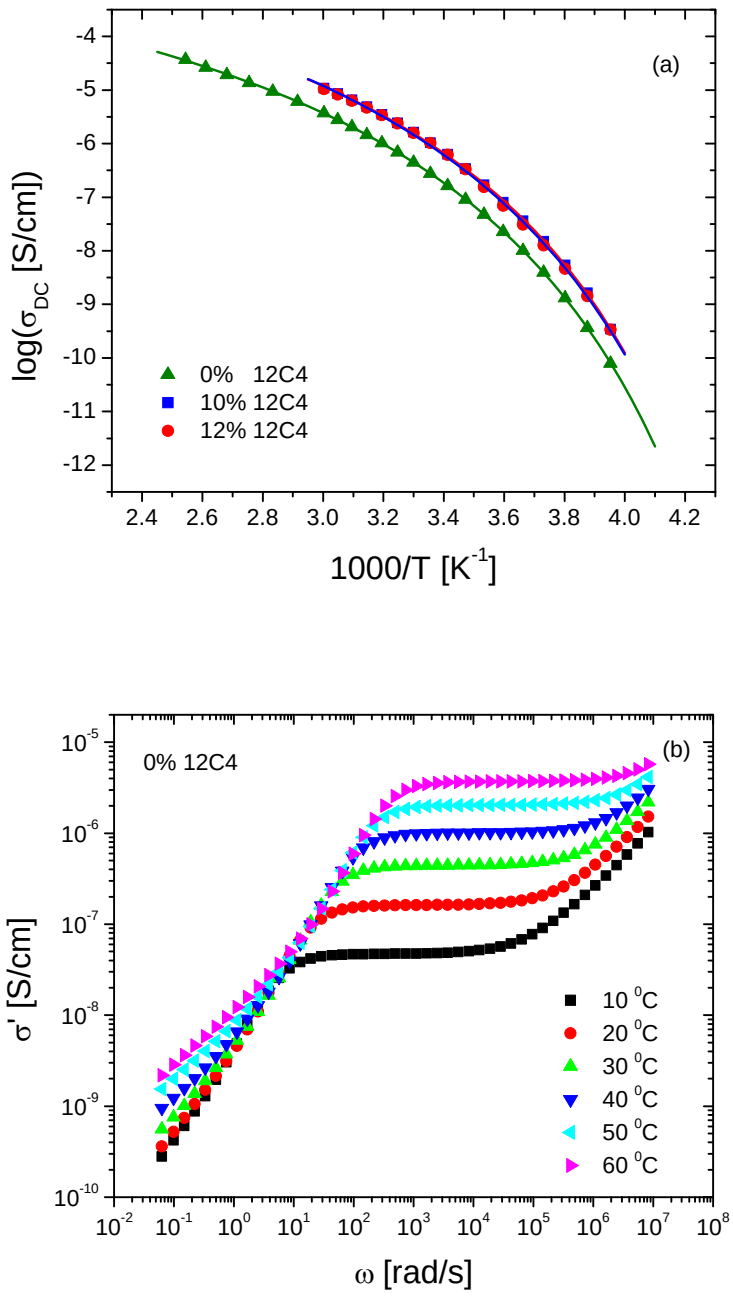

Figure 2.7. (a) Temperature dependence of ionic conductivity for PE600-0.5Li with 12C4 and without 12C4 (Lines indicate fits of the VFT equation (Eq. (2.2)) to the data) and (b) ac conductivity as a function of frequency at the several temperatures for PE600-0.5Li.

The fit parameters σ_0, T_0, and B are given in Table 2.2. This form was originally used to describe the viscosity of polymeric materials, where viscosity and conductivity are inversely related by the Walden relationship.[101]

Table 2.2. Parameters of the VFT equations for the DC conductivity and ion mobility.

Sample	DC conductivity			Ion mobility		
	$\log\sigma_0$ (S/cm)	B	T_0 (K)	$\log\mu_0$ ($cm^2V^{-1}S^{-1}$)	B	T_0 (K)
0% 12C4	-2.2	2.2	198	-2.8	1.4	206
10% 12C4	-1.9	2.0	199	-3.0	1.2	212
12% 12C4	-1.7	2.2	197	-2.6	1.3	210

The similar temperature dependences of viscosity, segmental motion and ionic conductivity strongly suggest that structural motions of the polymer are necessary for ionic motion leading to conduction. This confirms that in these ionomers there is strong coupling between ion transport and segmental motion which is observed in the derivative spectra of Fig. 2.5.

It is clear that an increase in the conductivity takes place in the ionomers containing crown ethers. However, in order to better understand the conduction mechanism, it is necessary to distinguish whether the increase in ionic conductivity is due to a larger fraction of conducting ions or to an increase in ion mobility, because conductivity depends on the number density of conducting ion as well as their mobility. The result is presented in the following section.

2-3.5. Electrode polarization model

The ionic conductivity can be separated into the contributions of conducting ion mobility and conducting ion concentration using a physical model of electrode polarization (EP) which was observed in the dielectric loss spectrum.[45-47] The EP occurs at low frequencies, where the transporting ions have sufficient time to polarize at the blocking electrodes during the cycle. That polarization manifests itself in (1) an increase in the effective capacitance of the cell (increasing the dielectric constant) and (2) a decrease in the in-phase part of conductivity, as the polarizing ions reduce the field experienced by the transporting ions. The polarization time scale when the conducting ions fully polarize at the electrode is

$$\tau_{EP} \equiv \frac{\varepsilon_{EP}\varepsilon_0}{\sigma_{DC}} \tag{2.5}$$

where ε_{EP} is the (considerably larger) effective permittivity after the electrode polarization is complete, ε_0 is the permittivity of vacuum, and σ_{DC} is the d.c. conductivity. The Macdonald and Coelho model[102,103] treats electrode polarization as a simple Debye relaxation

$$\varepsilon_{EP}^{*}(\omega) = \frac{\Delta\varepsilon_{EP}}{1 + i\omega\tau_{EP}} \tag{2.6}$$

where $\Delta\varepsilon_{EP} = \varepsilon_{EP} - \varepsilon_s$. The Debye relaxation makes it possible to determine τ_{EP} and ε_{EP} through fitting to the experimental data. The Macdonald and Coelho model then determines the mobility μ and the number density of conducting ions p from τ_{EP} and ε_{EP}:

$$\mu = \frac{eL^2\varepsilon_s}{4\varepsilon_{EP}\tau_{EP}kT} \tag{2.7}$$

$$p = \frac{4\varepsilon_0 kT}{\varepsilon_s}\left(\frac{\varepsilon_{EP}}{eL}\right)^2 \tag{2.8}$$

where L is the spacing between electrodes, e is the elementary charge, k is the Boltzmann constant, and T is absolute temperature.

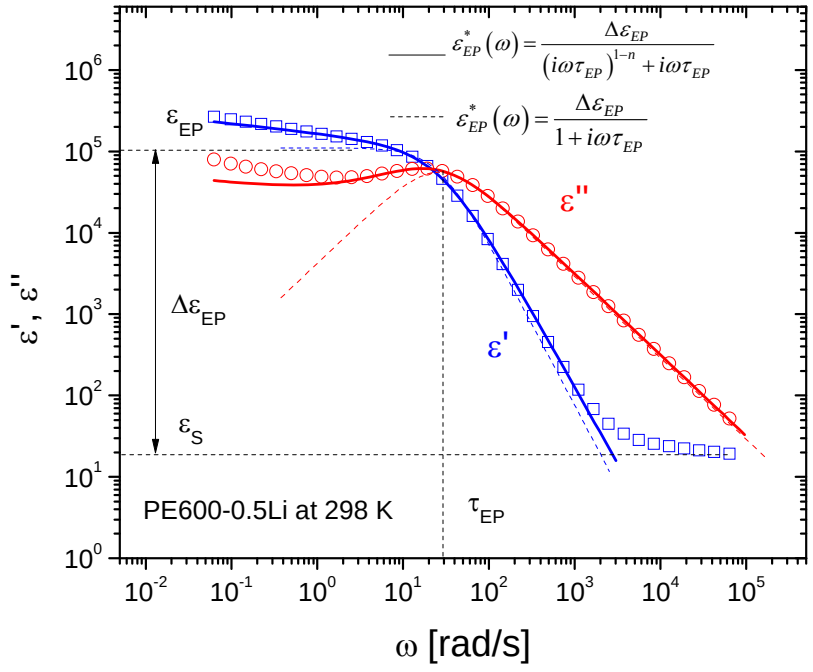

Figure 2.8. Dielectric constant and loss as a function of angular frequency at 298 K for PE600-0.5Li. Lines are fits of Eq. (2.6) (dash line) and Eq. (2.9) (solid line) with $n = 0.884$ to the data

The experimental data can be analyzed using an empirical modification of the Macdonald model[46,47]

$$\varepsilon^*_{EP}(\omega) = \frac{\Delta\varepsilon_{EP}}{(i\omega\tau_{EP})^{1-n} + i\omega\tau_{EP}} \tag{2.9}$$

Equation (2.9) provides a much better fit to the experiment data than the original Macdonald model (Eq. (2.6)) (see Fig. 2.8). The exponent n has been suggested to relate to electrode roughness $(0 < n \leq 1)$.[104] The ε' and ε'' data are fit to Eq (2.9) yielding ε_{EP} and τ_{EP}, from which Eq (2.7) and (2.8) are used to obtain μ and p. The Debye relaxation (Eq. (2.6)) is a special case of Eq. (2.9) with $n = 1$.

2-3.5.1. Conducting ion mobility

The ionic conductivity can be separated into the contributions of conducting ion mobility and conducting ion number density. The ion mobility determined from the EP model (Eq. (2.9)) is displayed in Fig. 2.9. To account for the ion mobility, we fit the results using a VFT equation.

$$\mu = \mu_{\infty} \exp\left(-\frac{B}{T - T_0}\right) \tag{2.10}$$

Fitting parameters for the ion mobility are shown in Table 2.1. As is the case of the ionic conductivity, ion mobility shows a VFT tendency with increasing temperature dependence. The VFT dependence of ion mobility reflects the coupling of segmental motion of polymer backbone and ion motion. As expected, the ion mobility of Li^+ in PE600 was improved by the addition of 12C4. At first glance it might seem that lithium-crown ether complexes should decrease ion mobility because of surrounding the cation with a large bulky group. The addition of crown ethers to ion-containing polymer system leads to a reduction in cation-anion interaction and thus promotes cation dissociation. As long as the system shows slightly weaker interaction between lithium ion and crown ether, the cation motion may be less suppressed while some enhancement of cation dissociation is maintained. This may be connected with ion transport mechanisms which are the free volume theory[105] and dynamic bond percolation model[106]. The proposed models

indicate that spaces or channels for ionic motion to move from site to site must form due to activated motions of the polymer host. In this case the crown ethers which can move a little, but only in a narrowly confined region in the polymer matrix are located at the fixed sites. The cations, assisted by the segmental motion of the polymer host, could exchange themselves between the nearest-neighbor crown ether molecules. This may provide a possible description of the enhanced ion mobility in these materials.

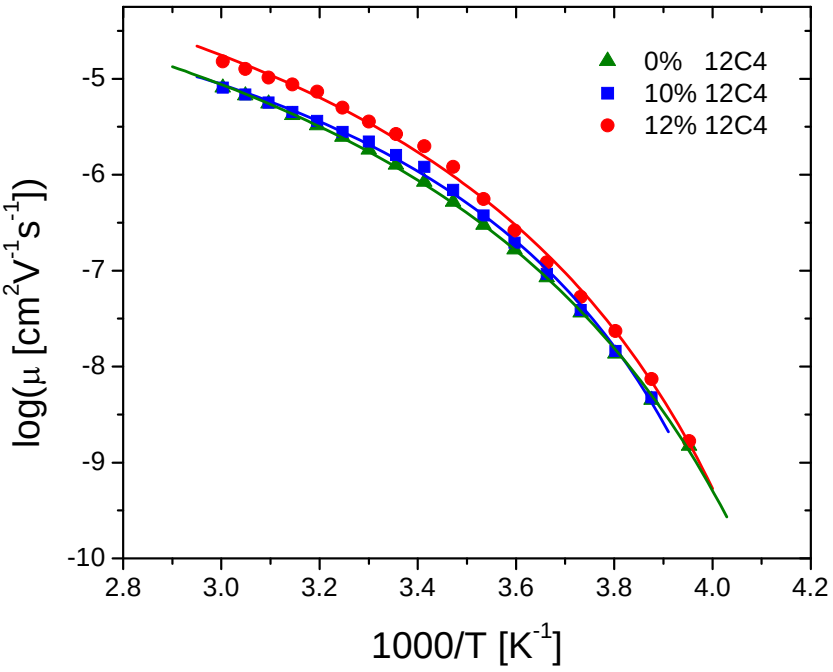

Figure 2.9. Ion mobility μ vs inverse temperature. Lines are fits of Eq. (2.10) to the data

2-3.5.2. Conducting ion concentration

Figure 2.10 shows conducting ion concentration in the ion-containing polymers, determined using the EP model. The result indicates that the addition of crown ether to PE600-0.5Li ionomer raises the number density of conducting ions.

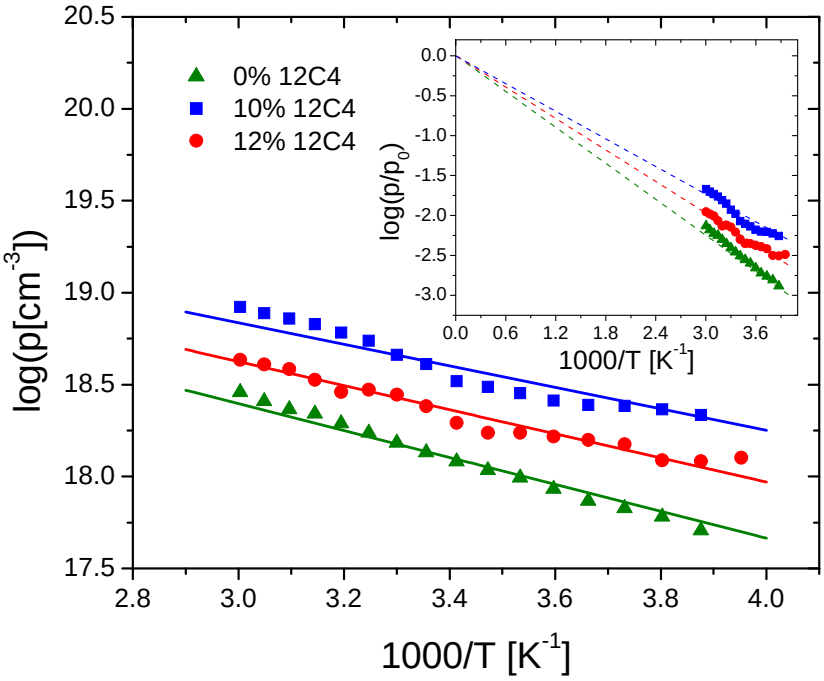

Figure 2.10. Conducting ion concentration p as a function of inverse temperature. The inset shows p divided by the total ion concentrations p_0. Lines are fits of Eq. (2.11) to the data.

The temperature dependence of conducting ion concentration for these ionomers is well described by an Arrhenius equation

$$p = p_\infty \exp\left(-\frac{E_a^p}{RT}\right) \tag{2.11}$$

where p_∞ is the conducting ion concentration as $T \to \infty$ and E_a^p is an activation energy for conducting ions. The Arrhenius temperature dependence indicates that the conducting ions will be fully dissociated at infinite temperature. The activation energy of the conducting ion concentration in these ionomers is associated with the binding energy of an ion pair because the main driving force for pair formation seems to be electrostatic attraction between cation and anion.[46]

Table 2.3. Fitting parameters for Eq. (2.11) for the conducting ion concentration.

Sample	Conducting ion concentration	
	$\log p_\infty$ (cm^{-3})	E_a^p (kJ/mol)
0% 12C4	20.6	14.0
10% 12C4	20.6	11.2
12%12C4	20.6	12.5

Arrhenius plots and corresponding fit parameters are displayed in Fig 2.10 and Table 2.3. The Arrhenius plots were fitted with the known total ion concentration ($p_0 \approx 3.9\times10^{20} cm^{-3}$) calculated from the stoichiometry.[47] Interestingly, the ionomer with crown ether shows a lower activation energy than that without crown ether. To explain this behavior, it was proposed that the activation energy of the sulfonated ionomer is simply described by the Coulomb energy[45,47]

$$E_a = \frac{q^2}{4\pi\varepsilon_0\varepsilon_s r} \tag{2.12}$$

The Coulomb equation suggests that E_a is directly related with the dielectric constant ε_s as well as the separation between cation and anion r. Not only PE600-0.5Li with crown ether showed higher ε_s, but also the systems might have longer r due to the formation of complex between Li ion and crown ether, than that without crown ether. Thus, the more the dielectric constant and the separation, the less the activation energy. This would lead to a decrease in the activation energy with increasing the amount of crown ether. However, this simple model is not sufficient to describe higher conducting ion concentration in 10%_12C4, and additional effects resulting from ionic interaction play an important role in determining the fraction of conducting ions in terms of the amount of crown ether. Further investigations are necessary to clarify this point.

2-4. Summary

In order to see whether the presence of the crown ether would give rise to a conductivity enhancement as well as account for its mechanism, we studied dielectric properties and ion conduction of PEO-based polyester copolymer ionomers with and without crown ether using dielectric relaxation spectroscopy. It appears that the addition of crown ether to PE600-0.5Li improves its ionic conductivity from 10^{-7} to 10^{-6} S/cm at room temperature. The dc conductivity is strongly coupled with segmental motion of polymer chain so that the temperature dependency of ionic conductivity followed VFT behavior. A physical model of EP makes it possible for dc conductivity to be separated into (1) conducting ion mobility and (2) conducting ion concentration. The observation of EP in dielectric loss spectra indicated that lithium ions bound with 12C4 is faster than those which show strong affinity with PEO. The result was also observed

in the temperature dependency of conducting ion mobility. A reduction in interaction between sulfonate anion and lithium cation owing to the incorporation of crown ether leads to a slight improvement of the ion mobility. The formation of Li-complex with crown ether causes a large increase in the static dielectric constant, suggesting that most ions form separated ion pairs. The increase of the static dielectric constant boosts the number density of conducting ions, and this has the largest contribution to increased conductivity. Nevertheless, it is not clear at this stage why such small quantities of crown ether should enhance conducting ion concentration. It is necessary to independently investigate conducting ion concentration and mobility using complementary method.

2-5. Future work

Dielectric relaxation spectroscopy was used here to understand ion transport properties of these ionomers, which are conducting ion mobility and concentration. The fact that very small fractions of the ions participated in ion conduction indicates a very large fraction of ions bound in ion pairs or larger aggregates. To fully understand the basic mechanism of ion transport in these materials, it is necessary to investigate the distribution of ion states, which are ion pairs, triples, and quadrupoles. The *ab initio* calculation, a powerful tool for studying intermolecular interaction[107,108], quantifies interaction energies between cations and anions in different polar media, enabling a detailed estimation of interaction energies of each ion state. Furthermore, the number density of ion pair can be not only described by the Onsager equation, but also compared with conducting ion concentration.

Chapter 3

Double a.c. Hall Effect Measurement of the Number Density of Charge Carriers and their Mobility

In this chapter we focus on how to directly measure conducting ion number density p and conducting ion mobility μ, making use of a Hall Effect which is the production of a potential difference, called the Hall voltage, across a conductor in which an electric current perpendicularly flows in the presence of a magnetic field. The Hall voltage can be measured by using either d.c. or a.c. sources to supply the sample current and the magnetic field. We not only analyze fundamental theories about the two Hall measurements to apply the concepts to ion-containing polymer systems but also investigate the necessary apparatuses and technologies for measuring the Hall Effect of the low-mobility systems. On the basis of the theoretical and experimental backgrounds we will fully explore the possibilities of measuring ionic Hall Effect using a double a.c. Hall measurement.

3-1. d.c. Hall Effect

3-1.1. Basic equations for d.c. Hall Effect

In 1879 Hall discovered Hall effect, which uses a combination of electric and magnetic fields to determine the number density p, mobility μ and the sign of the charge carrier in semiconductors.[109] The magnetic field applied to a conductor, perpendicular to the current flow direction, produces a Hall voltage perpendicular to both the magnetic field and the current direction. The measured Hall voltage determines the Hall coefficient, which makes it possible to distinguish the carrier sign, the concentration of charge carriers, and their mobilities.[110]

The Hall Effect has been extensively used for the characterization of classical semiconductor materials (doped Si, GaAs) where it enables determination of mobility and concentration of electrons or holes.[110] Figure 3.1 shows the Hall Effect in a p-type semiconductor. The applied current I and measured voltage along the x-direction, V_ρ, are given by

$$I = qwdpv_x = qwdp\varepsilon_x\mu_p \tag{3.1}$$

$$V_\rho = \frac{\rho sI}{wd} \tag{3.2}$$

where q is the carrier's charge (usually $\pm e$), ρ is the resistivity, s is the voltage measuring length (see Fig. 3.1), p and μ_p are the number of holes and the hole mobility, and v_x and ε_x are the carrier velocity and electric field along x-direction. If a uniform magnetic field B is applied perpendicular to the direction in which holes drift in a p-type bar, the motion of holes tends to be deflected due to the total force, which is given by the vector expression:

$$F = q(\varepsilon + v \times B) \tag{3.3}$$

The important result of Eq. (3.3) is that in the y-direction there is no net force on the holes since no current can flow in that direction and $F_y = F_E + F_{LO} = 0$. In order to maintain a steady state flow of holes down the length of the bar, the electric field ε_y must balance the product Bv_x:

$$\varepsilon_y = Bv_x = \frac{BI}{qwdp} \tag{3.4}$$

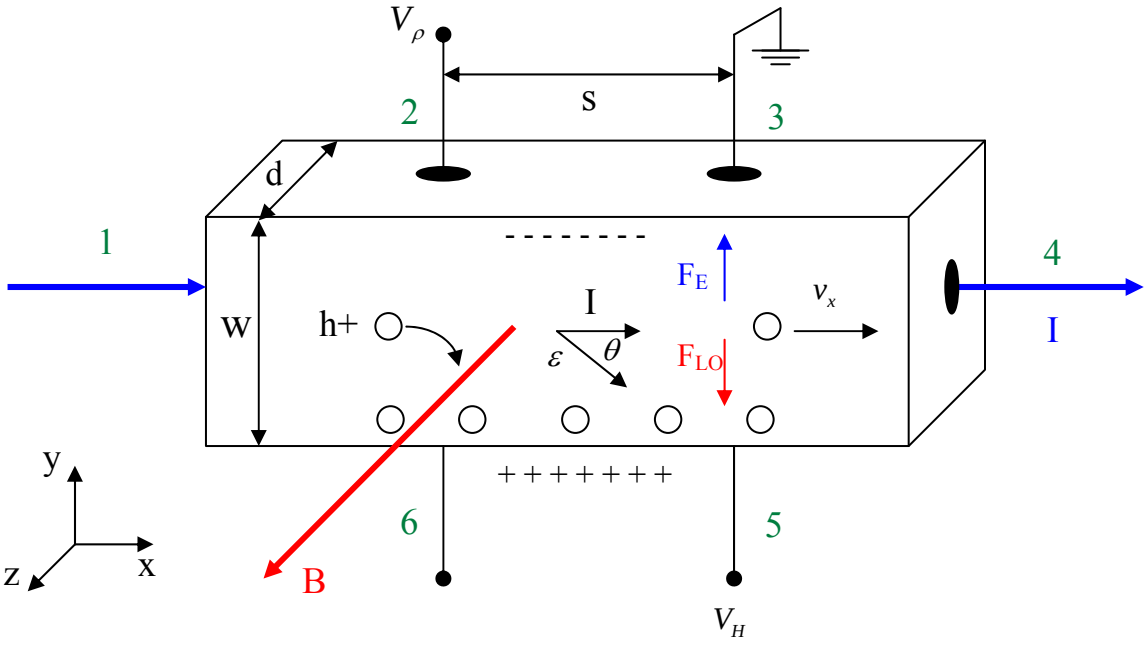

Figure 3.1. Schematic illustrating the Hall Effect in a p-type sample

The electric field in the y-direction produces the Hall voltage V_H

$$\int_0^{V_H} dV = V_H = -\int_w^0 \varepsilon_y dy = -\int_w^0 \frac{BI}{qwdp} dy = \frac{BI}{qdp} \tag{3.5}$$

The Hall coefficient R_H is defined as a ratio

$$R_H = \frac{V_H d}{BI} = \frac{1}{qp} \tag{3.6}$$

The Hall voltage and the Hall coefficient give the number density of holes p and electrons n:

$$p = \frac{1}{qR_H}; n = -\frac{1}{qR_H} \tag{3.7}$$

The sign of the Hall voltage and the Hall coefficient determine the sign of the charge carrier, as illustrated in Figure 3.2.

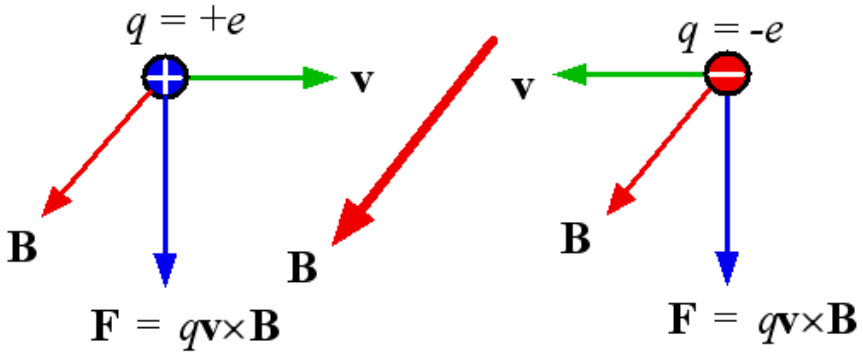

Figure 3.2. Different signs of charge carriers give different signs of Hall voltage

The mobility μ_p is simply the ratio of the Hall coefficient and the resistivity:

$$\mu_p = \frac{\sigma}{qp} = \frac{R_H}{\rho} \tag{3.8}$$

In addition, the Hall angle θ between the current and the net electric field is

$$\tan(\theta) = \frac{\varepsilon_y}{\varepsilon_x} = B\mu_p; \theta = \arctan\left(B\mu_p\right) \tag{3.9}$$

by combining Eq. (3.1) and (3.4). The Hall angle depends only on carrier mobility and magnetic field. At weak magnetic field, this reduces to

$$\theta \approx B\mu_p \tag{3.10}$$

It is interesting to note that the Hall Effect demonstrates a current deflection effect. When both holes and electrons are present, the Hall coefficient in Eq. (3.6) becomes[111]

$$R_H = \frac{\left(p - b^2 n\right) + \left(\mu_n B\right)^2 \left(p - n\right)}{q\left[\left(p + bn\right)^2 + \left(\mu_n B\right)^2 \left(p - n\right)^2\right]} \tag{3.11}$$

This result is relatively complex and depends on the mobility ratio $b = \mu_n / \mu_p$ and on the magnetic field strength B. Eq. (3.7) is derived under simplifying assumptions of energy-independent scattering mechanisms. With this assumption relaxed, the expression for the hole and electron densities become[111,112]

$$p = \frac{r}{qR_H}; n = -\frac{r}{qR_H} \tag{3.12}$$

where r is the Hall scattering factor, defined by $r = <\tau^2> / <\tau>^2$, with τ being the relaxation time between carrier collisions. The scattering factor depends on the energy distribution of the relaxation times. This energy distribution is a function of the scattering processes such as acoustic phonon, ionized impurities, or neutral impurities.[113] Thus the quantity r depends on the scattering mechanism and generally lies between 1 and 2. The scattering factor is also a function of magnetic field and temperature and can be determined by measuring R_H in the high magnetic field limit:

$$r = \frac{R_H(B)}{R_H(B = \infty)} \tag{3.13}$$

3-1.2. Measurement Procedures

In many cases the specific resistivity and the Hall Effect of a conducting material are measured by cutting a sample in the form of a bar as illustrated in Fig. 3.1. The specific resistivity is derived from the potential drop between the points 2 and 3 or 6 and 5 in the absence of the magnetic field (see Fig. 3.1). On the other hand, as the current flows into 1 and out of 4, the Hall voltage is measured between 2 and 6 or between 3 and 5 in the presence of a magnetic field. The equations derived in Section. 3-1.1 apply for this geometry.

Hall samples come in two basic geometries: (1) bridge type and (2) lamella type. The choice of the bar sample shape shown in Fig. 3.1 is sometimes not recommended because of contact resistance fluctuations with time, temperature and other variables. To ease the contact problem, the Hall bridge has extended arms as shown in Fig. 3.3(a).[114] The lamellar specimen may be of arbitrary shape, but a symmetrical configuration is preferred as shown in Fig. 3.3(b) to (c). For the lamellar shape it is important for the contacts to be small and to be placed as close to the periphery as possible.

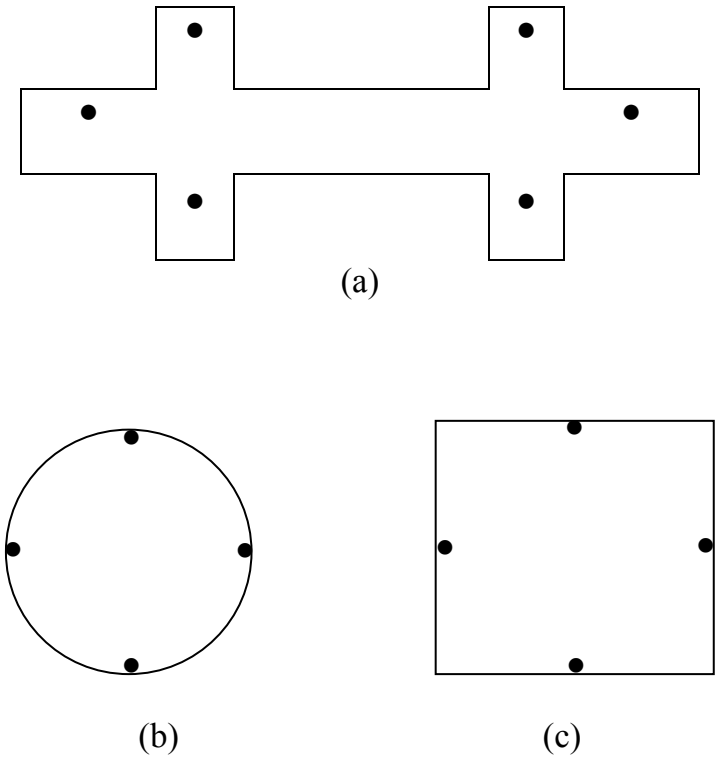

Figure 3.3. (a) Bridge-type Hall configuration, (b) and (c) lamella-type Hall configuration

Furthermore, the theoretical foundation of the Hall measurement evaluation for irregularly shaped samples is based on conformal mapping developed by van der Pauw.[115,116] He introduced how the resistivity, carrier concentration, and mobility of a flat sample of arbitrary shape can be determined without knowing the current pattern if the following conditions are fulfilled: (1) the contacts are at the circumference of the sample, (2) the contacts are sufficiently small, (3) the sample is uniformly thick, and (4) the sample surface is singly connected, i.e., the sample does not contain isolated holes.

A variety of procedures have been used to make electrical contacts to samples used for Hall Effect measurements. In most cases the making of reliable ohmic contacts is one of the problems which should be solved for reasonable measurements. Pressure contacts are common for room temperature measurements on metals as well as used for high temperature Hall measurements.[117] For high temperature application or reactive materials, graphite is used for pressure contacts.[117] Soldered contacts using indium or low temperature indium eutectic alloys can be used for making reliable contacts to low temperature bandgap semiconductors.[117] The soldering should preferably be done in an oxygen-free environment in order to prevent the formation of a cold-solder joint. Furthermore, painted contacts made of a metallic powder such as silver or gold in a colloidal organic binder are used for basic contacts on small bandgap semiconductors. For organic materials gold or platinum electrodes are deposited at a thickness of 50-100 nanometers by vacuum evaporation or sputtering through a shadow mask.

In an ideal case these Hall electrodes are point contacts placed on an equipotential plane so that $V_H = 0$ for $B = 0$: in reality there is usually a misalignment potential V_0 between them. The potential measured between the Hall electrodes for $B \neq 0$ is, therefore, the sum of the misalignment potential and of the Hall voltage, $V_m = V_H + V_0$. The misalignment potential can be

eliminated by measuring V_m for two opposite orientation equal amplitude magnetic fields while keeping all other parameters constant.

3-1.3. Limitation of d.c. Hall Effect for Ionic Hall Effect

The basic concepts for d.c. Hall Effect in semiconductors should be, in the same way, of great help in the understanding of ion transport phenomena in polymer complexes. Moreover, elementary theoretical approaches for the estimation of Hall Effect in ionic solutions have been reported. Friedman[118] introduced a Brownian motion based model of ionic mobility where the Hall coefficient is directly proportional to the imposed magnetic field strength and inversely proportional to the coefficient of friction between ions and solvent. The results indicated that the Hall Effect is large enough to be measurable, at least for solutions of quite mobile ions.

However, measuring the Hall Effect of ions in a solid with a direct current is very difficult because the mobility of ionic carriers is less than one-millionth of the highest mobility of electrons or holes in semiconductors.[118] Owing to the small mobility, the Hall angle is also small and therefore the Hall field is even smaller. The small Hall voltage determined in this manner may be in serious error where the electromotive force due to temperature gradients is large compared with the Hall voltage.[119] Polarization effects due to the space charge near the electrodes under an electric field also causes additional difficulties in the Hall effect measurements.[120] Furthermore, in the case of materials for high-speed devices having many conducting layers, the straightforward d.c. Hall Effect techniques can be of only very limited use to analyze the materials.[121] Under d.c. measurements it is very unlikely to apply a uniform magnetic force upon the overall sample. Also it is difficult to analyze the data performing depth profiling because space charges can accumulate or deplete across the sample layer boundaries depending on the

relative strength of their respective electrochemical potential. For these reasons we need a highly sensitive Hall Effect measurement for the realization of the measurement of the ionic Hall Effect, even if there is practical theoretical knowledge which has been reported in ionic systems.

3-2. a.c. Hall Effect

Mobility measurements of charge carriers in conducting materials are complicated by two experimental factors: (1) the high impedance level of the samples, (2) the difficulties of applying Ohmic electrodes to the material.[122] Non-Ohmic contacts result in a space charge effect within the material that distorts and decreases the effective electric field in the region of the Hall electrodes. An a.c. Hall measurement method can provide an excellent solution to avoid these problems.

The a.c. Hall voltage can be measured by using (1) a.c. current and d.c. magnetic field, (2) d.c. current and a.c. magnetic field, or (3) a.c. current and a.c. magnetic field of different frequencies. Olson and Wertz[123] reported that a Hall Effect apparatus with method (1) has increased sensitivity compared with conventional d.c. Hall measurements. Using the same method Macdonald and Robinson[124] avoided space charge difficulties in colored alkali halides by applying an alternating voltage and measuring with an a.c. Hall voltage detector. Method (2) is rarely used due to the a.c. magnet requirement. Method (3) is the best detection system because the Hall voltages are measured at the sum and difference frequencies of alternating current and a.c. magnetic field.

In this double a.c. method, the current I at frequency ω_1 and the magnetic field B at frequency ω_2 are expressed by

$$I = I_0 \cos(\omega_1 t) \tag{3.14}$$

$$B = B_0 \cos(\omega_2 t) \tag{3.15}$$

The Hall voltage V_H oscillates at two frequencies $\omega_+ = \omega_1 + \omega_2$ or $\omega_- = \omega_1 - \omega_2$ is

$$\begin{aligned} V_H &= (R_H / d) IB = (R_H / d) I_0 \cos(\omega_1 t) B_0 \cos(\omega_2 t) \\ &= (R_H / 2d) I_0 B_0 \left[\cos((\omega_1 + \omega_2)t) + \cos((\omega_1 - \omega_2)t) \right] \end{aligned} \tag{3.16}$$

The Hall signal is selected and amplified at both the sum frequency ω_+ and the difference frequency ω_- with the aid of lock-in amplifiers in order to isolate those two signals from the other components of the Hall signal.

In 1950, Russell and Wahlig[125] proposed the first alternating current methods for more precise determination of Hall coefficients. An alternating current and an alternating magnetic field of a different frequency are passed through a sample to create a Hall voltage along the third axis that consists of two parts, one part oscillating at the sum of the two input frequencies and the other part oscillating at the difference of the two input frequencies. Pell and Sproul[126] introduced a sensitive recording a.c. Hall Effect apparatus. It is especially optimized for measuring Hall voltage in samples of very low conductivity. The Hall voltage is measured by use of a magnetic field reversed periodically, an oscillator, and an a.c. amplifier and phase sensitive detector with a recorder output. Gobrecht et al.[127] have also extended the utility of such a.c. Hall measurements to samples with high resistances. An a.c. generator which provides the current drives an amplifier which also has a compensator to eliminate the misalignment potential. The a.c. Hall output voltage is applied to a preamplifier which also serves as impedance transformer. After amplification, the Hall output voltage is detected synchronously by an amplifier which provides the proper phase compensation with respect to the current. The alternating magnetic field has also been accomplished by rotating a washer-shaped sample in a d.c. magnetic field.[128] In this manner we can simulate an a.c. magnetic field without the penalties imposed by the impedance and time constants of the magnet and its power supply. A similar improved apparatus adapted to the

measurement of low mobility and high resistivity systems was described by Hermann and Ham.[129] The sample is rotated at 20 Hz in a static magnetic field by a synchronous motor. The current to the sample is a 13.33 Hz signal and the magnetic field and the current are in phase with the line frequency. A phase-sensitive synchronous amplifier is used to detect the Hall voltage at 33.33 Hz. Its bandwidth is reduced to 0.05 Hz and the misalignment voltage which appears at 13.33 Hz is rejected. This double modulation method was also applied to high impedance photoconductors in order to do photo-Hall mobility measurements. The magnetic field is modulated by rotating the sample in the field and the density of charge carriers is modulated by a chopped light beam directed through an aperture in the center of the magnet pole while a d.c. electric field is applied to it along a direction perpendicular to the magnetic field.

These a.c. Hall measurements show more advantages than the original d.c. measurement. The a.c. excitation current reduces both thermoelectric and galvanomagnetic effects in the sample as well as space charge effects at the electrical contacts.[130] The use of an a.c. current also allows the use of lock-in amplifiers with filters which reject all frequency components except the desired Hall component.[128] The multiple commutations of current and magnetic field polarities necessary to eliminate thermoelectric and thermomagnetic errors and misalignment voltages which appear in d.c. measurements[112,117] are not required with the double a.c. method.[131] The theory of the a.c. Hall Effect in inhomogeneous solids is also developed using the effective-medium theory.[132,133] The results describe the frequency dependence of the effective conductivity, the Hall conductivity, the Hall mobility and the Hall coefficient.

In 1964, Greenfield[134] accurately measured a Hall coefficient of 9 liquid metals using the double a.c. method. Kyser and Thompson[135] extended the double a.c. method to metal-ammonia solutions. With the double a.c. method, Read and Katz[136] measured the ionic Hall effect in single crystal NaCl at high temperature. Kanede et al.[120] and Newman et al.[137] measured the ionic Hall effect in solid electrolyte $RbAg_4I_4$ and $C_5H_6NAg_5I_6$. For dilute solution, Bellissent et al.[138] and

Meton et al.[139] reported the experimental quantity of ionic Hall effect and Levitt[140] calculated ionic mobilities and transport numbers from Shockley's equation. Modern work[141-146] also shows rather convincingly that the double a.c. method can be extremely sensitive. For example, Kasai et al.[145] have established a highly sensitive and precise double a.c. Hall Effect apparatus for a wide range of specimen resistance, from 100 mΩ to 100 GΩ. Therefore, the a.c. Hall effect system combined with both theoretical works and the advanced a.c. techniques has potential to measure the ionic Hall Effect in single ion conducting ionomers. The estimated result can play an important role in comprehensive understanding of ion transport in ion-containing polymers as providing the ion density and mobility.

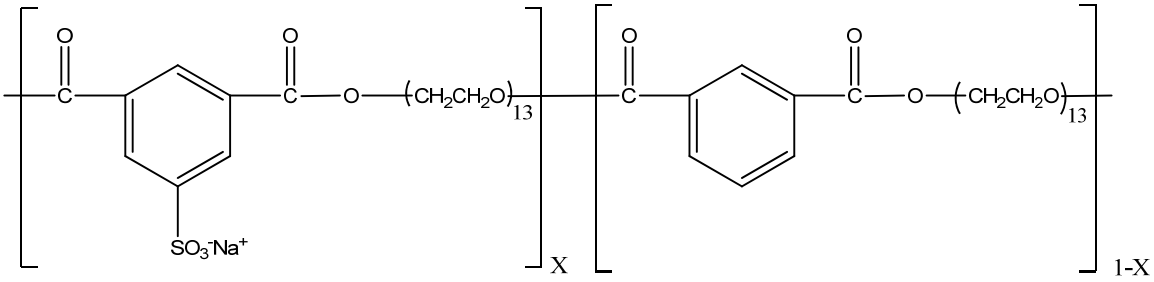

Figure 3.4. Chemical structure of the polyester copolymer ionomer PE600-xNa (x=0.1)

3-3. Results and discussion

To study the ionic Hall Effect of ion-containing polymer, we choose a polyester copolymer ionomer based on poly(ethylene oxide) (PEO). It is a single-ion (Na^+) conductor, with sulfonate anions covalently bound to the polymer chains.[147] The structure of the ionomer is shown

in Fig. 3.4: the materials are similar to those studied in ref. 39, where ion content was varied by changing the length of the PEO subchains. Here, instead, ion content is systematically varied by changing the ratio of ionic to non-ionic isophthalate groups while keeping a fixed PEO segment molecular weight of 600 (13 EO repeat units).

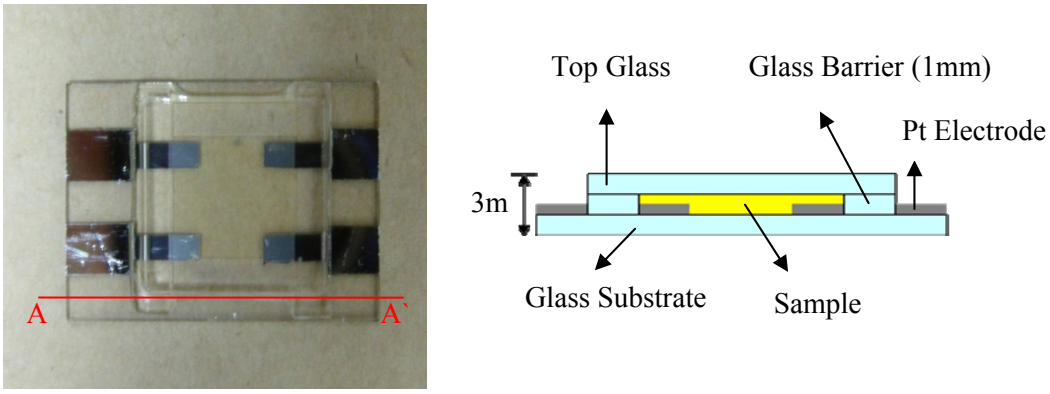

(a) (b)

Figure 3.5. Hall sample cell: (a) top view with a glass substrate and four Pt electrodes (b) cross section along cut A-A`

Samples for Hall measurements were placed onto a sample cell which consisted of a substrate and four electrodes. (see Fig. 3.5) The sample cell was glass and the electrodes were deposited on a glass substrate using a sputtering method. To study the influence of electrodes on the Hall measurements, we also demonstrated different kinds and shapes of electrodes like Fig. 3.6. Using an I-V Curve Tracer which shows the relationship between current and voltage, we found that Pt electrodes showed ohmic contact with the sample, but Cu electrodes showed non-ohmic contact with one. We may explain this result from a contact issue between electrode and sample. Both the electrode and sample have their own work function, $q\Phi$, which is the minimum

energy required for an electron or ion to escape from the sample into vacuum.[148] In ionic systems this is simply the ion pairing energy. When a metal with work function $q\Phi_m$ is brought in contact with a sample having a work function $q\Phi_s$, potential barriers arise in the metal-sample contacts. The work function of Cu is 4.65 eV and that of Pt is 5.65 eV.[149] Their differences have an influence on the contact between the metal and sample. The potential barriers also depend on interfacial states between electrode and sample.[150] The nature of the actual interface may be strongly influenced by chemical interactions between the two materials.

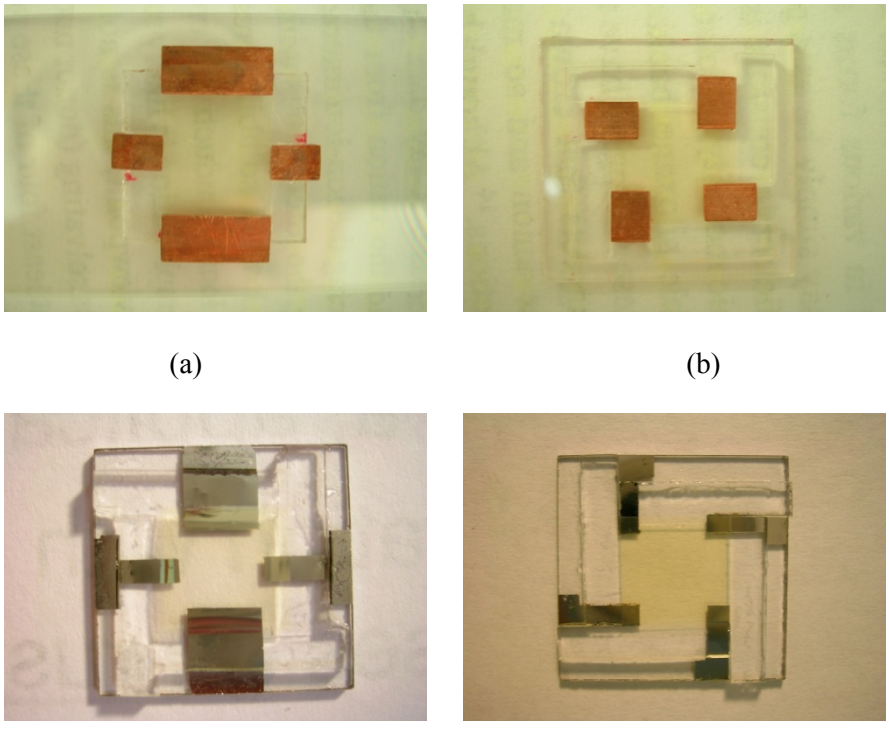

(a) (b)

(c) (d)

Figure 3.6. Four kinds of sample cells: (a) and (b) Cu electrodes, (c) and (d) Pt electrodes

Before a top glass plate was placed on the sample, it was dried in a vacuum oven at 373 K for one day. The glass barrier was used to control the sample thickness at 1 mm. A Spectromagnetic Industries d.c. Hall Measurement system was used to measure the Hall voltage. To measure conductivity and Hall coefficient, the sample cell was attached to a sample holder, as shown in Fig 3.7. We used a van der Pauw geometry which was mentioned in Sec. 3-1.2. In the basic van der Pauw contact arrangement, the four contacts made to the sample are numbered clockwise in ascending order when the sample is viewed from Fig. 3.8 with the magnetic field perpendicular to the sample.

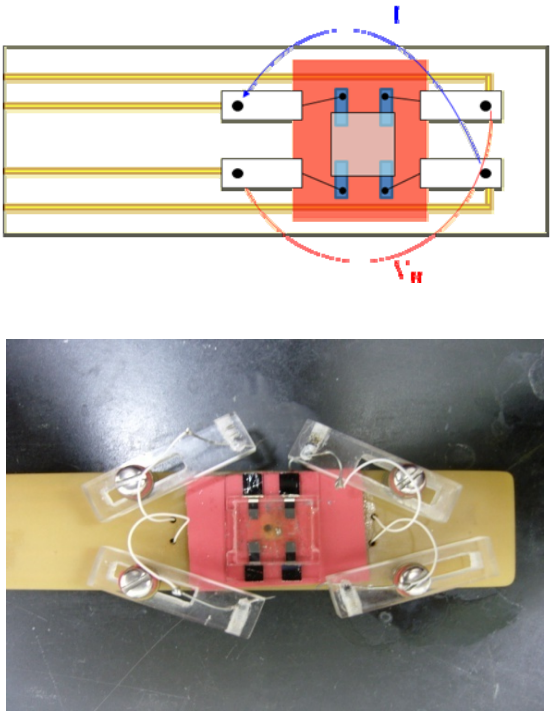

Figure 3.7. Schematic illustrating the Hall sample holder with four-point probe.

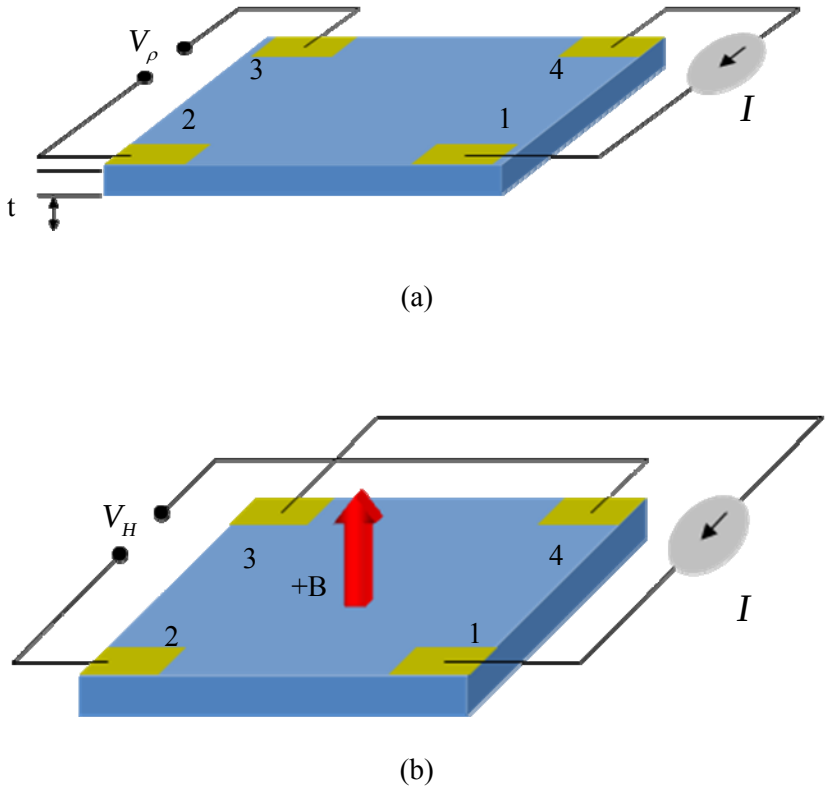

Figure 3.8. Measuring resistivity (a) and Hall coefficient (b) using a van der Pauw geometry

The Hall voltage measurements are further complicated by an ohmic voltage contribution that arises from the misalignment of the Hall probes. This large ohmic voltage contribution must be eliminated by making voltage measurements in the two oppositely oriented magnetic field directions $\left(V_m(+), V_m(-)\right)$ shown in Fig. 3.9 and subtracting the two readings:[151] $V_H = \left[V_m(+) - V_m(-)\right]/2$.

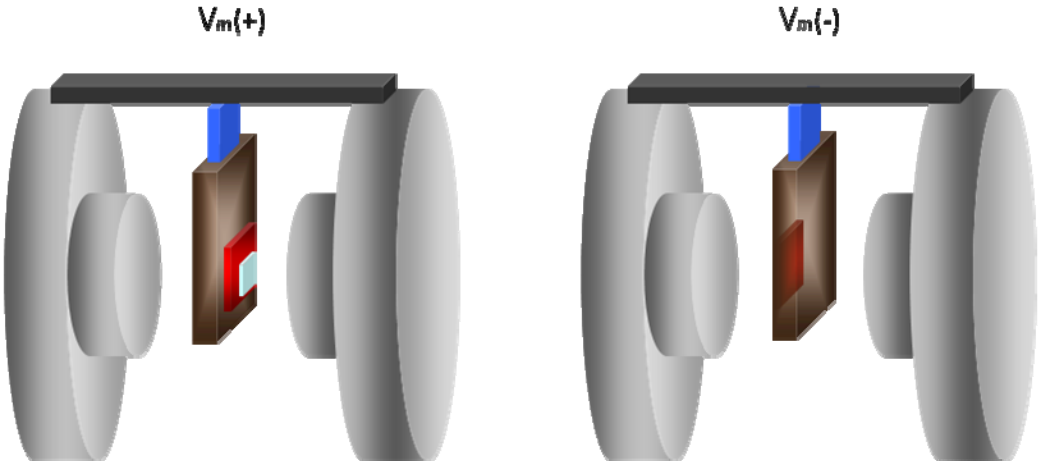

(a) (b)

Figure 3.9. Measured voltage: (a) $V_m(+)$ along + direction of magnetic field, (b) $V_m(-)$ along – direction of magnetic field.

The measurements were conducted in d.c. current $I = 0.3\,\mathrm{mA}$ and d.c. magnetic field $B = 0.5\,\mathrm{T}$ at room temperature. Figure 3.10 shows the time dependency of voltage V_H measured between the Hall contacts under those conditions. The measured voltage is around $0.7685\,\mathrm{V}$. Its magnitude may come from misalignment of the electrodes because the two pairs are not perfectly perpendicular. The + direction voltage $V_M(+)$ is changing with time a lot. This result presumably reflects that we measured some electronic drift. It is quite clear that the d.c. Hall measurement cannot measure the Hall voltage of the ion-containing polymer system. In order to measure its Hall voltage we need to change from + direction to – direction very rapidly. In practice the method is done more easily in the frequency domain with oscillating electric field and oscillating magnetic field. That will be the double a.c. Hall Effect measurement discussed in Section 3-2.

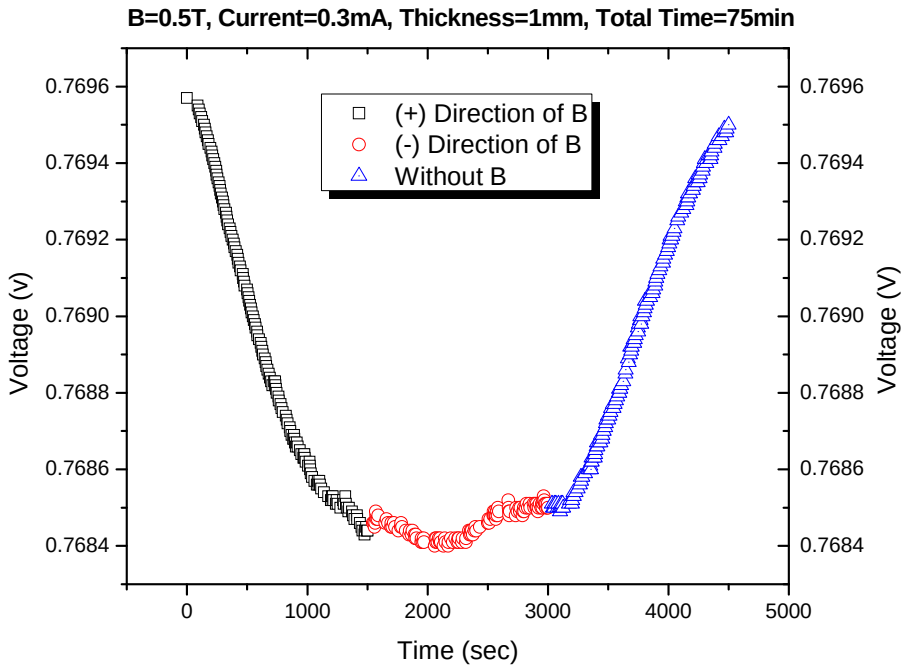

Figure 3.10. Voltage between the Hall contacts V_H recorded as a function of time for PEO-10%Na at $I = 0.3mA$, $B = 0.5T$, and $T = 298K$.

3-4. Summary

In addition to the dielectric spectroscopy measurement, we suggested the Hall Effect which is a manifestation of the Lorentz force on an ensemble of charged particles constrained to move in a given direction and subjected to a transverse magnetic field in order to understand ion transport and interaction of mobile ions with ion-containing polymers. These understandings require to precisely quantify two vital quantities, ion concentration and ion mobility, in various

conditions. The double a.c. Hall effect method introduced in this chapter is designed to measure both number density of conducting ions and their mobility.

We defined and discussed the fundamental equations of both d.c. and a.c. Hall Effect, which give some ideas to figure out how the Hall Effect systems can directly measure concentration of charge carriers and their mobilities. Moreover, we investigated not only the essential components of apparatus for Hall Effect measurements but also the reported previous and modern works which succeeded to measure ionic Hall Effect in liquid solutions, dilute electrolytes, or solid electrolytes.

With these theoretical and experimental results, we tried to estimate Hall voltage of PE600-0.1Na using d.c. Hall measurement. The results indicate that this technique may not be useful to measure Hall voltage of ion-containing polymer system with low mobility. Therefore, we need highly sensitive Hall Effect measurement for the realization of the measurement of the ionic Hall Effect. The double a.c. Hall Effect measurement is ideal for samples with charge carrier mobility too low for the d.c. Hall Effect measurement. All in all, we believe that our work provides new pathways for understanding the ion transport behavior of ion-containing polymer system and hope that this will drive additional experimental research in this area.

3-5. Future Work

1. We are preparing to use a double a.c. Hall Effect measurement system supplied by LakeShore Cryotronics of Westerville.[152] Their small electromagnet is suitable for our purpose. Driven with 35 V input, this magnet can produce magnetic field strengths of order 2 T. This system also makes it possible to get quite sinusoidal magnetic field at frequencies less than 1 Hz.

Moreover, we can even control temperature. The block diagram of our system is shown in Fig. 3.11.

2. With the new double a.c. Hall Effect system, we will observe the ionic Hall Effect of ion-containing polymer systems. For this experiment, the Hall data will be obtained over a wide temperature range from the near glass transition temperature of the sample to the high temperature (120 ^{0}C). The carrier density p and its mobility μ_p can be extracted from the Hall measurements. Thus we can show the temperature dependence of p and μ_p and also obtain activation energy for ion conduction in the system. These results can compare with the results by dielectric spectroscopy method.

3. When an electric field ε_x is applied in the x direction, each carrier experiences a net force $-q\varepsilon_x$ from the field. This force may be insufficient to alter appreciably the random path of an individual carrier: each group of carriers drifts with a different drift velocity. In crossed electric and magnetic fields the magnetic forces acting on carriers moving with different velocities. Therefore, the Hall electric field, ε_y, as defined in Eq. (3.4) cannot balance the magnetic forces, Bv_x, for each group of carriers. For carriers drifting faster as a result of the external electric field, the Hall electric field is too weak to balance the magnetic forces, and these carriers also drift in the direction of resultant magnetic forces. For carriers drifting slower, the Hall electric field overcompensates the action of the magnetic forces, and these carriers drift also as a result of the Hall electric field. These results cannot satisfy the condition of a zero transverse current. The existence of the transverse current components means the existence of a kind of current deflection effect, mentioned in Section. 3-1.1. With the double a.c. method we may be able to explain this process by taking into account the scattering of carriers. We need to take account of the distribution of velocities and the interactions of the charge carriers with impurities,

defects, and lattice thermal vibration of material. The Hall system with a frequency response makes it possible to study the temperature dependence of the Hall scattering factor r as discussed in Section. 3-1.1 because we can control the relaxation time between carriers collision, τ. This result will be quite useful to figure out ion transport mechanisms with scattering process in ion-containing polymer systems.

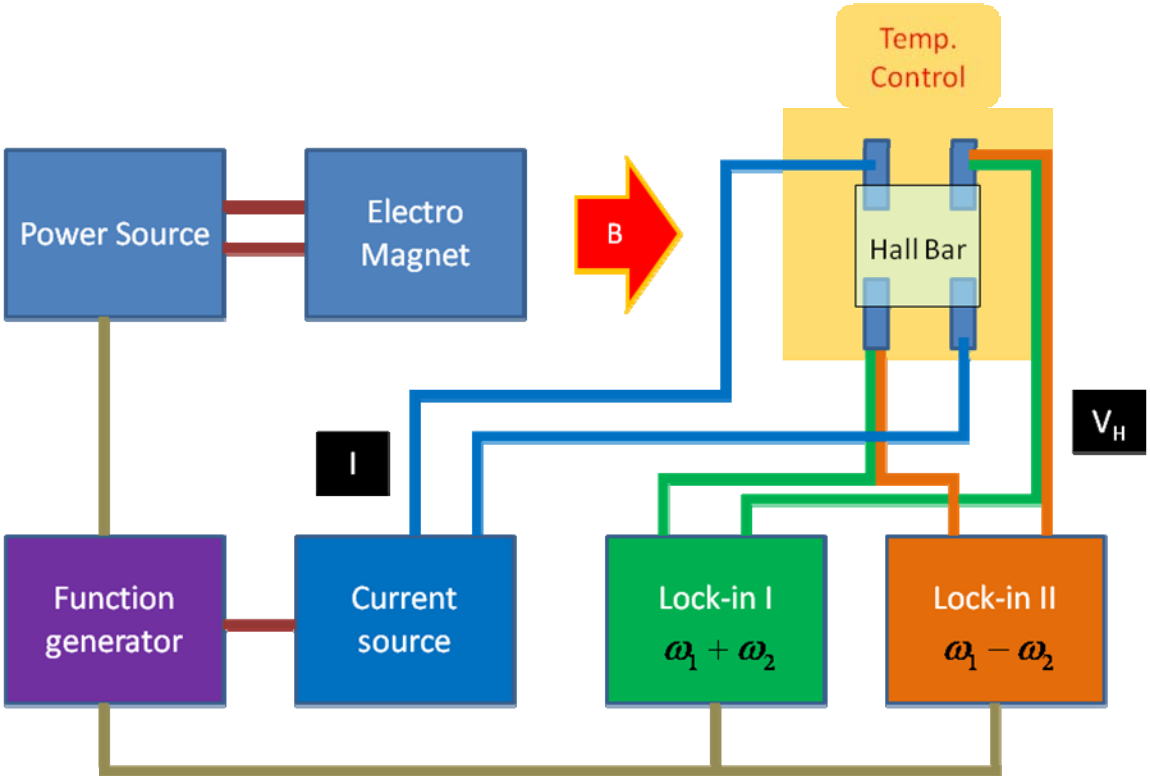

Figure 3.11. Block Diagram for double a.c. Hall Effect measurements

Reference

1. Whittingham, M. S. Materials Challenges Facing Electrical Energy Storage. *MRS Bulletin* **33**, 411-419 (2008).
2. Tarascon, J. M. & Armand, M. Issues and challenges facing rechargeable lithium batteries. *Nature* **414**, 359-367 (2001).
3. Armand, M. & Tarascon, J. M. Building better batteries. *Nature* **451**, 652-657 (2008).
4. Blythe, T. & Bloor, D. *Electrical Properties of Polymers* (Cambridge University Press, Cambrideg, 2005).
5. Yoshimatsu, I., Hirai, T. & Yamaki, J.-i. Lithium Electrode Morphology during Cycling in Lithium Cells. *J. Electrochem. Soc.* **135**, 2422-2427 (1988).
6. Owen, J. R. Rechargeable Lithium Batteries. *Chem. Soc. Rev.* **26**, 259-267 (1997).
7. Meyer, W. H. Polymer Electrolytes for Lithium-Ion Batteries. *Adv. Mater.* **10**, 439-448 (1998).
8. Wright, P. V. Electrical Conductivity in Ionic Complexs of Poly(ethylene oxide). *Br. Polym. J.* **7**, 319 (1975).
9. R. Edward Barker, J. Mobility and Conductivity of Ions in and into Polymeric Solids. *Pure & Appl. Chem.* **46**, 157-170 (1976).
10. Faraday, M. *Experimental Research in Electricity* (Taylor and Francis, London, 1839).
11. Fenton, D. E., Parker, J. M. & Wright, P. V. Complexes of alkali metal ions with poly(ethylene oxide). *Polymer* **14**, 589 (1973).
12. Armand, M. B., Chabagno, J. M. & Duclot, M. *Fast Ion Transport in Solids* (eds. Vashishta, P., Mundy, J. N. & Shenoy, G. K.) (North-Holland, Amsterdam, 1979).

13. Ratner, M. A., Johansson, P. & Shriver, D. F. Polymer Electrolytes:Ionic Transport Mechanisms and Relaxation Coupling. *MRS Bulletin*, 31-37 (2000).

14. Ferry, J. D. *Viscoelastic properties of polymers* (Wiley, New York, 1980).

15. Scrosati, B. & Vincent, C. A. Polymer Electrolyte: The Key to Lithium Polymer Batteries. *MRS Bulletin*, 28-30 (2000).

16. Osaka, T. & Datta, M. *Energy Storage Systems for Electronics* (Gordon and Breach Science, 2000).

17. Tsunemi, K., Ohno, H. & Tsuchida, E. A mechanism of ionic conduction of poly (vinylidene fluoride)-lithium perchlorate hybrid films *Electrochim. Acta* **28**, 833-837 (1983).

18. Bruce, P. G. & Vincent, C. A. Polymer Electrolytes. *J. Chem. Soc. Faraday Trans.* **89**, 3187 (1993).

19. Papke, B. L., Ratner, M. A. & Shrive, D. F. Vibrational sepctroscopy and structure of polymer electrolytes, poly(ethylene oxide) complexes of alkali metal salts. *J. Phys. Chem. Solid.* **42**, 493-500 (1981).

20. Berthier, C., Gorecki, W., Minier, M., Armand, M. B., Chabagno, J. M. & Rigaud, P. Microscopic Investigation of Ionic Conductivity in Alkali Metal Salts-poly(ethylene oxide) Adducis. *Solid State Ionics* **11**, 91-95 (1983).

21. MacGlashan, G. S., Andreev, Y. G. & Bruce, P. G. Structure of the polymer electrolyte poly(ethylene oxide)$_6$:LiAsF$_6$. *Nature* **398**, 792-794 (1999).

22. Christie, A. M., Lilley, S. J., Staunton, E., Andreev, Y. G. & Bruce, P. G. Increasing the conductivity of crystalline polymer electrolytes. *Nature* **433**, 50-53 (2005).

23. Zhang, C., Gamble, S., Ainsworth, D., Slawin, A. M. Z., Andreev, Y. G. & Bruce, P. G. Alkali metal crystalline polymer electrolytes. *Nature Mater.* **8**, 580-584 (2009).

24. Bruce, P. G. Coordination chemistry in the solid state. *Phil. Trans. R. Soc. Lond. A* **354**, 415-436 (1996).

25. Takeoka, S., Ohno, H. & Tsuchida, E. Recent Advancement of Ion-conductive Polymers. *Polym. Adv, Technol.* **4**, 53-73 (1992).

26. R. Edward Barker, J. & Sharbaugh, A. H. Ionic Conduction in Polymer Films and Related Systems. *J. Polym. Sci. C*, 139-152 (1965).

27. Porter, C. H. & Boyd, R. H. A Dielectric Study of the Effects of Melting on Molecular Relaxation in Poly (ethylene oxide) and Polyoxymethylene. *Macromolecules* **4**, 589-594 (1971).

28. Yano, S., Rahalkar, R. R., Hunter, S. P., Wang, C. H. & Boyd, R. H. Studies of Molecular Relaxation of Poly(propylene Oxide) Solutions by Dielectric Relaxation and Brillouin Scattering. *J. Polym. Sci. Polym. Phys,* **14**, 1877-1890 (1976).

29. Pettit, L. D. & Bruckenstein, S. The Thermodynamics of Ion Association in Solution. I. An Extension of the Denison-Ramsey Equations. *J. Am. Chem. Soc.* **88**, 4783-4789 (1966).

30. Scrosati, B. *Applications of electroactive polymers* (Chapman & Hall, London, 1993).

31. Thomas, K. E., Sloop, S. E., Kerr, J. B. & Newman, J. Comparison of lithium-polymer cell performance with unity and nonunity transference numbers. *J. Power Sources* **89**, 132-138 (2000).

32. Sun, X.-G., Hou, J. & Kerr, J. B. Comb-shaped single ion conductors based on polyacrylate ethers and lithium alkyl sulfonate. *Electrochim. Acta* **50**, 1139-1147 (2005).

33. Sun, X.-G. & Kerr, J. B. Synthesis and Characterization of Network Single Ion Conductors Based on Comb-Branched Polyepoxide Ethers and Lithium Bis(allylmalonato)borate. *Macromolecules* **39**, 362-372 (2006).

34. Doyle, M., Fuller, T. F. & Newman, J. The importance of the lithium ion transference number in lithium/polymer cells *Electrochim. Acta* **39**, 2073-2081 (1994).

35. Mehta, M. A. & Fujinami, T. Novel inorganic-organic polymer electroltyes-preparation and properties. *Solid State Ionics* **113-115**, 187-192 (1998).

36. Mehta, M. A., Fujinami, T. & Inoue, T. Boroxine ring containing polymer electrolytes. *J. Power Sources* **81-82**, 724-728 (1999).

37. Mehta, M. A., Fujinami, T., Inoue, S., Matsushita, K., Miwa, T. & Inoue, T. The use of boroxine rings for the development of high performance polymer electrolytes. *Electrochim. Acta* **45**, 1175-1180 (2000).

38. Sun, X. & Angell, A. "Acid-in-chain" versus "base-in-chain" anionic polymer electrolytes for electrochemical devices. *Electrochim. Acta* **46**, 1467-1473 (2001).

39. Sun, X.-G., Xu, W., Zhang, S.-S. & Angell, C. A. Polyanionic electrolytes with high alkali ion conductivity. *J. Phys.: Condens. Matter* **13**, 8235-8243 (2001).

40. Xu, W., Sun, X.-G. & Angell, C. A. Anion-trapping and polyanion electrolytes based on acid-in-chain borate polymers. *Electrochim. Acta* **48**, 2255-2266 (2003).

41. Zhou, G.-b., Khan, I. M. & Smid, J. Solvent-Free Cation-Conducting Polysiloxane Electrolytes with Pendant Oligo(oxyethy1ene) and Sulfonate Groups. *Macromolecules* **26**, 2202-2208 (1993).

42. Snyder, J. F., Ratner, M. A. & Shriverz, D. F. Ion Conductivity of Comb Polysiloxane Polyelectrolytes Containing Oligoether and Perfluoroether Sidechains. *J. Electrochem. Soc.* **150**, A1090-A1094 (2003).

43. Watanabe, M., Suzuki, Y. & Nishimoto, A. Single ion conduction in polyether electrolytes alloyed with lithium salt of a perfluorinated polyimide. *Electrochim. Acta* **45**, 1187-1192 (2000).

44. Dou, S., Zhang, S., Klein, R. J., Runt, J. & Colby, R. H. Synthesis and Characterization of Poly(Ethylene Glycol)-Based Single-Ion Conductors. *Chem. Mater.* **18**, 4288-4295 (2006).

45. Klein, R. J., Zhang, S., Dou, S., Jones, B. H., Colby, R. H. & Runt, J. Modeling electrode polarization in dielectric spectroscopy: Ion mobility and mobile ion concentration of single-ion polymer electrolytes. *J. Chem. Phys.* **124**, 144903 (2006).

46. Fragiadakis, D., Dou, S., Colby, R. H. & Runt, J. Molecular Mobility, Ion Mobility, and Mobile Ion Concentration in Poly(ethylene oxide)-Based Polyurethane Ionomers. *Macromolecules* **41**, 5723-5728 (2008).

47. Fragiadakis, D., Dou, S., Colby, R. H. & Runt, J. Molecular mobility and Li+ conduction in polyester copolymer ionomers based on poly(ethylene oxide). *J. Chem. Phys.* **130**, 064907 (2009).

48. Ratner, M. A. & Nitzan, A. Fast ion conduction: some theoretical issues. *Solid State Ionics* **28-30**, 3-33 (1988).

49. Miyamoto, T. & Shibayama, K. Free-volume model for ionic conductivity in polymers. *J. Appl. Phys.* **44**, 5372-5376 (1973).

50. Williams, M. L., Landel, R. F. & Ferry, J. D. The Temperature Dependence of Relaxation Mechanisms in Amorphous Polymers and Other Glass-forming Liquids. *J. Am. Chem. Soc.* **77**, 3701-3707 (1955).

51. Cohen, M. H. & Turnbull, D. Molecular Transport in Liquids and Glasses. *J. Chem. Phys.* **31**, 1164-1169 (1959).

52. Adam, G. & Gibbs, J. H. On the Temperature Dependence of Cooperative Relaxation Properties in Glass-Forming Liquids. *J. Chem. Phys.* **43**, 139-146 (1965).

53. Mott, N. F. & Davis, E. A. *Electronic processes in ionic crystals* (Oxford : Clarendon Press, Oxford, 1948).

54. Druger, S. D., Ratner, M. A. & Nitzan, A. Polymeric Solid Electrolytes: Dynamic Bond Percolation and Free Volume Models for Diffusion. *Solid State Ionics* **9-10**, 1115-1120 (1983).

55. Druger, S. D., Nitzan, A. & Ratner, M. A. Dynamic bond percolation theory: A microsocpic model for diffusion in dynamically disordered systems. I. Definition and one-dimensional case. *J. Chem. Phys.* **79**, 3133-3142 (1983).

56. Ratner, M. A. & Nitzan, A. Conductivity in Polymer Ionics. Dynamic Disorder and Correlation. *Faraday Discuss. Chem. Soc.* **88**, 19-42 (1989).

57. Nitzan, A. & Ratner, M. A. Conduction in Polymers: Dynamic Disorder Transport. *J. Phys. Chem.* **98**, 1765-1775 (1994).

58. Druger, S. D. Ionic transport in polymer electrolytes based on renewing environments. *J. Chem. Phys.* **100**, 3979-3984 (1994).

59. Lonergan, M. C., Nitzan, A., Ratner, M. A. & Shriver, D. F. Dynamically disordered hopping, glass transition, and polymer electrolytes. *J. Chem. Phys.* **103**, 3253-3261 (1995).

60. McQuarrie, D. A. *Statistical Mechanics* (Harper & Row, New York, 1976).

61. Onsager, L. Electric Moments of Molecules in Liquids. *J. Am. Chem. Soc.* **58**, 1486 (1936).

62. Davies, G. W. *Ion Association* (Butterworths, Washington, 1962).

63. Fuoss, R. M. & Kirkwood, J. G. Electrical Properties of Solids. VIII. Dipole Moments in Polyvinyl Chloride-Diphenyl Systems. *J. Am. Chem. Soc.* **63**, 385-394 (1941).

64. Radhakrishna, S. & Daud, A. *Solid State Materials* (Springer-Verlag, New Delhi, 1991).

65. Bjerrum, N. Ionic association. I. Influence of ionic association on the activity of ions at moderate degrees of association. *Kgl. Danske Videnskab. Selskab. Math.-fys. Medd. [9]* **7**, 1-48 (1926).

66. Fuoss, R. M. & Kraus, C. A. Properties of electrolytic solutions III The dissociation constant. *J. Am. Chem. Soc.* **55**, 1019-1028 (1933).

67. Fuoss, R. M. & Kraus, C. A. Properties of electrolytic solutions IV The conductance minimum and the formation of triple ions due to the action of coulomb forces. *J. Am. Chem. Soc.* **55**, 2387-2399 (1933).

68. MacCallum, J. R., Tomlin, A. S. & Vincent, C. A. An Investigation of the Conducting Species in Polymer Electrolytes. *Eur. Polym. J.* **22**, 787-791 (1986).

69. Kakihana, M., Schantz, S. & Torell, L. M. Raman-Spectroscopic Study of Ion-Ion Interaction and Its Temperature-Dependence in a Poly(Propylene-Oxide)-Based $NaCF_3SO_3$-Polymer Electrolyte. *J. Chem. Phys.* **92**, 6271-6277 (1990).

70. Kakihana, M., Schantz, S., Torell, L. M. & Stevens, J. R. Dissociated Ions and Ion Ion Interactions in Poly(Ethylene Oxide) Based $NaCF_3SO_3$ Complexes. *Solid State Ionics* **40-1**, 641-644 (1990).

71. Schantz, S. On the Ion Association at Low Salt Concentrations in Polymer Electrolytes - a Raman-Study of $NaCF_3SO_3$ and $LiClO_4$ Dissolved in Poly(Propylene Oxide). *J. Chem. Phys.* **94**, 6296-6306 (1991).

72. Petersen, G., Jacobsson, P. & Torell, L. M. A Raman-Study of Ion Polymer and Ion Ion Interactions in Low-Molecular-Weight Polyether-$LiCF_3SO_3$ Complexes. *Electrochim. Acta* **37**, 1495-1497 (1992).

73. Leveque, M., Lenest, J. F., Gandini, A. & Cheradame, H. Cationic Transport Numbers in Polyether-Based Networks Containing Lithium-Salts. *J. Power Sources* **14**, 27-30 (1985).

74. Bruce, P. G., Hardgrave, M. T. & Vincent, C. A. The Determination of Transference Numbers in Solid Polymer Electrolytes Using the Hittorf Method. *Solid State Ionics* **53-6**, 1087-1094 (1992).

75. Stolwijk, N. A., Wiencierz, M. & Obeidi, S. Mass and charge transport in the PEO-NaI polymer electrolyte system: effects of temperature and salt concentration. *Faraday Discussions* **134**, 157-169 (2007).

76. Bohmer, R., Jeffrey, K. R. & Vogel, M. Solid-state LiNMR with applications to the translational dynamics in ion conductors. *Prog. Nucl. Magn. Reson. Spectrosc.* **50**, 87-174 (2007).

77. Judeinstein, P., Reichert, D., deAzevedo, E. R. & Bonagamba, T. J. NMR Multi-Scale Description of Ionic Conductivity Mechanisms Inside Polymer Electrolytes. *Acta Chim. Slov.* **52**, 349-360 (2005).

78. Sun, X. G., Kerr, J. B., Reeder, C. L., Liu, G. & Han, Y. B. Network single ion conductors based on comb-branched polyepoxide ethers and lithium bis(allylmalonato)borate. *Macromolecules* **37**, 5133-5135 (2004).

79. Blonsky, P. M., Shriver, D. F., Austin, P. & Allcock, H. R. Polyphosphazene Solid Electrolytes. *J. Am. Chem. Soc.* **106**, 6854-6855 (1984).

80. Killis, A., Nest, J.-F. L., Gandini, A. & Cheradame, H. Ionic Conductivity of Polyether-Polyurethane Networks Containing Alkali Metal Salts. An Analysis of the Concentration Effect. *Macromolecules* **17**, 63-66 (1984).

81. Weston, J. E. & Steele, B. C. H. Effects of Inert Fillers on the Mechanical and Electrochemical Properties of Lithium Salt-poly(ethylene oxide) polymer electrolytes. *Solid State Ionics* **7**, 75-79 (1982).

82. Pedersen, C. J. The Discovery of Crown Ethers. *Science* **241**, 536-540 (1988).

83. Hiraoka, M. *Crown Ethers and Analogous Compounds* (Elsevier, New York, 1992).

84. Pedersen, C. J. Cyclic Polyethers and Their Complexes with Metal Salts. *J. Am. Chem. Soc.* **89**, 7017-7036 (1967).

85. Kaplan, M. L., Rietman, E. A., Cava, R. J., Holt, L. K. & Chandross, E. A. Crown Ether Enhancement of Ionic Conductivity in a Polymer-salt System. *Solid State Ionics* **25**, 37-40 (1987).

86. Kaplan, M. L., Reitman, E. A. & Cava, R. J. Solid polymer electrolytes: attempts to improve conductivity. *Polymer* **30**, 504-508 (1989).

87. Nagasubramanian, G. & Stefano, S. D. 12-Crown-4 Ether-Assisted Enhancement of Ionic Conductivity and Interfacial Kinetics in Polyethylene Oxide Electrolytes. *J. Electrochem. Soc.* **137**, 3830-3835 (1990).

88. Nagasubramanian, G., Attia, A. I. & Halpert, G. Effects of 12-Crown-4 Ether on the Electrochemical Performance of CoO2 and TiS2 Cathodes in Li Polymer Electrolyte Cells. *J. Electrochem. Soc.* **139**, 3043-3046 (1992).

89. Morita, M., Tanaka, H., Ishikawa, M. & Matsuda, Y. Effects of crown ethers on the electrochemical properties of polymeric solid electrolytes consisting of poly(ethylene oxide)-grafted poly(methylmethacrylates). *Solid State Ionics* **86-88**, 401-405 (1996).

90. Izatt, R. M., Bradshaw, J. S., Nielsen, S. A., Lamb, J. D. & Christensen, J. J. Thermodynamic and Kinetic Data for Cation-Macrocycle Interactiont. *Chem. Rev.* **85**, 271-339 (1985).

91. Inoue, Y. & Gokel, G. W. *Cation Binding by Macrocycles: complexation of cationic species by crown ethers* (Marcel Dekker, Inc., New York, 1990).

92. Newman, D. S., Hazlett, D. & Mucker, K. F. Crown ether solid electrolytes with mobile halide ions. *Solid State Ionics* **3/4**, 389-392 (1981).

93. Weber, E., Toner, J. L., Goldberg, I., Vogtle, F., Laidler, D. A., Stoddart, J. F., Bartsch, R. A. & Liotta, C. L. *Crown Ethers and Analogs* (Wiley, 1989).

94. Dou, S. C., Zhang, S. H., Klein, R. J., Runt, J. & Colby, R. H. Synthesis and characterization of poly(ethylene glycol)-based single-ion conductors. *Chemistry of Materials* **18**, 4288-4295 (2006).

95. McMurry, J. *McMurry Organic Chemistry 3* (Brooks/Cole, Paific Grove, 1992).

96. Pauer, F., Rocha, J. & Stalke, D. Synthesis and Crystal Structure of Bis(12-crown-4)lithium Bis[N, N'-bis(trimethylsilyl)benzensulphinamidino]lithiate(1-); the First Observation of Three Different Lithium-7 Environments in High-resolution Solid-state NMR Spectroscopy. *J. Chem. Soc., Chem. Commun.*, 1477-1479 (1991).

97. Kremer, F. & Schonhals, A. *Broadband Dielectric Spectroscopy* (Springer-Verlag, 2002).

98. Wubbenhorst, M. & van Turnhout, J. Analysis of complex dielectric spectra. I. One-dimensional derivative techniques and three-dimensional modelling. *J. Non-Cryst. Solids* **305**, 40-49 (2002).

99. McCRUM, N. G., Read, B. E. & Williams, G. *Anelastic and Dielectric Effects in Polymeric Solids* (Dover Publications, Inc, New York, 1991).

100. Morita, M., Hayashida, H. & Matsuda, Y. Effects of Crown Ether Addition to Organic Electrolytes on the Cycling Behavior of the TiS_2 Electrode. *J. Electrochem. Soc.* **134**, 2107-2111 (1987).

101. Lonergan, M. C., Nitzan, A., Ratner, M. A. & Shriver, D. F. Dynamically Disordered Hopping, Glass-Transition, and Polymer Electrolytes. *J. Chem. Phys.* **103**, 3253-3261 (1995).

102. Macdonald, J. R. Theory of ac Space-Charge Polarization Effects in Photoconductors, Semiconductors, and Electrolytes. *Phys. Rev.* **92**, 4 (1953).

103. Coelho, R. On the static permittivity of dipolar and conductive media-an educational approach. *J. Non-Cryst. Solids* **131-133**, 1136-1139 (1991).

104. Pajkossy, T. s. Impedance spectroscopy at interfaces of metals and aqueous solutions — Surface ruoughness, CPE and related issues. *Solid State Ionics* **176**, 1997-2003 (2005).

105. David Turnbull & Cohen, M. H. Free-Volume Model of the Amorphous Phase: Glass Transition. *J. Chem. Phys.* **34**, 120-125 (1961).

106. S. D. Druger, M. A. Ratner & Nitzan, A. Polymeric Solid Electrolytes: Dynamic Bond Percolation and Free Volume Models for Diffusion. *Solid State Ionics* **9 & 10**, 1115-1120 (1983).

107. Buckingham, A. D., Fowler, P. W. & Hutson, J. M. Theoretical studies of van der Waals molecules and intermolecular forces. *Chem. Rev.* **88**, 963-988 (1988).

108. Chaasiski, G. & Szczesniak, M. M. State of the Art and Challenges of the ab Initio Theory of Intermolecular Interactions. *Chem. Rev.* **100**, 4227-4252 (2000).

109. Hall, E. H. On a new action of the magnet on electric currents. *American Journal of Mathematics* **2**, 287-292 (1879).

110. Schroder, D. K. *Semiconductor material and device characterization* (IEEE Press, 2006).

111. Smith, R. A. *Semiconductors* (Cambridge University Press, Cambridge, 1959).

112. Putley, E. H. *The Hall Effect and Related Phenomena* (Butterworths, London, 1960).

113. Popovic, R. S. *Hall Effect Devices* (Institute of Physics Publishing, Philadepohia, 2004).

114. *Standard Method for Measuring Hall Mobility and Hall Coefficient in Extrinsic Semiconductor Single Crystals* (1996 Annual Book of ASTM Standards, West Conshohocken, 1996).

115. Pauw, L. J. v. d. A method of measuring specific resistivity and hall effect of discs of arbitrary shape. *Philips. Res. Repts* **13**, 1-9 (1958).

116. Pauw, L. J. v. d. A method of measuring the resistivity and Hall coefficient on lamellae of arbitrary shape. *Philips Tech. Rev.* **20**, 220-224 (1958).

117. Wieder, H. H. *Laboratory Notes on Electrical and Galvanomagnetic Measurements* (Elsevier, New York, 1979).

118. Friedman, H. L. Calculation of the Hall Effect in Ionic Solutions. *J. Phys. Chem.* **69**, 2617-2628 (1965).

119. Leverton, W. F. & Dekker, A. J. Hall coefficient and resistivity of thin films of antimony prepared by distillation. *Phys. Rev.* **80**, 732-736 (1950).

120. Kaneda, T. & E., M. Hall Effect of Silver Ions in $RbAg_4I_5$ Single Crystals. *Phys. Rev. Lett.* **29**, 937-939 (1972).

121. How, H., Tian, W. & Vittoria, C. AC-Hall Effect in multilayered semiconductors. *J. Lightwave Technol.* **15**, 1006-1011 (1997).

122. Eisele, I. & Kevan, L. Double Modulation Method for Hall Effect Measurements on Photoconducting Materials. *Rev. Sci. Instrum.* **43**, 189-194 (1972).

123. Olson, E. E. & Wertz, J. E. A high impedance ac Hall effect apparatus. *Rev. Sci. Instrum.* **41**, 419-421 (1970).

124. Macdonald, J. R. & Robinson, J. E. AC Hall and Magnetostrictive Effects in Photoconducting Alkali Halides. *Phys. Rev.* **95**, 44-50 (1954).

125. Russell, B. R. & Wahlig, C. A new method for the measurement of hall coefficients. *Rev. Sci. Instrum.* **21**, 1028-1029 (1950).

126. Pell, E. M. & Sproull, R. L. Sensitive recording alternating-current hall effect appartus. *Rev. Sci. Instrum.* **23**, 548-552 (1952).

127. Gobrecht, H., Franke, K. H., Niemeck, F. & Boeters, K. E. *Z. Angew. Phys.* **13**, 261 (1961).

128. Ryan, F. M. Rotating sample method for measuring the hall mobility. *Rev. Sci. Instrum.* **33**, 76-79 (1962).

129. Hermann, A. M. & Ham, J. S. Apparatus for the measurement of the Hall Effect in semiconductors of low mobility and high resistivity. *Rev. Sci. Instrum.* **36**, 1553-1555 (1965).

130. Clement, V., Ravaine, D., Deportes, C. & Billat, R. Measurement of hall mobilites in AgPO3-AgI glasses. *Solid State Ionics* **28-30**, 1572-1578 (1988).

131. Lundberg, B. & Backstrom, G. Hall voltage and magnetoresistance of Bi measured by a sum frequency method in a belt apparatus. *Rev. Sci. Instrum.* **43**, 872-875 (1972).

132. Fishchuk, I. I. The AC magnetoresistance in inhomogeneous solids. *J. Phys.: Condens. Matter* **4**, 8045-8052 (1992).

133. Fishchuk, I. I. Theory of the AC Hall effect in polycrystalline semiconductors. *J. Phys.: Condens. Matter* **6**, 2747-2750 (1994).

134. Greenfield, A. J. Hall coefficient of liquid metals. *Phys. Rev.* **135**, A1589-A1595 (1964).

135. Kyser, D. S. & Thompson, J. C. Measurement of the Hall effect in metal-ammonia solutions. *J. Chem. Phys.* **42**, 3910-3918 (1965).

136. Read, P. L. & Katz, E. Ionic hall effect in sodium chloride. *Phys. Rev. Lett.* **5**, 466-468 (1960).

137. Newman, D. S., Frank, C., Matlack, R. W., Twining, S. & Krishnan, V. The ionic hall effect in the solid eletrolyte $C_5H_6NAg_5I_6$. *Electrochim. Acta* **22**, 811-814 (1977).

138. Bellissent, M.-C., Gerard, P., Longevialle, C., Meton, M., Pich, M. & Morand, G. Experimental Measurements of the Hall Effect in Very Dilute Solutions. *J. Electrochem. Soc.: Electrochemical Science* **118**, 1944-1950 (1971).

139. Meton, M. & Gerard, P. Hall effect in dilute electrolytes. *Chem. Phys. Lett.* **44**, 582-585 (1976).

140. Levitt, L. S. Ionic transference numbers and mobilities from hall effect measurement of electrolytic solutions. *Electrochim. Acta* **21**, 239-240 (1976).

141. McLevige, W. V., Chatterjeet, P. K. & Streetman, B. G. Versatile double AC Hall effect system for profiling impurities in semiconductors. *J. Phys. E: Sci. Instrum.* **10**, 335-337 (1977).

142. R H Friend & Bett, N. Design of an alternating current source for resistivity and Hall effect measurements. *J. Phys. E: Sci. Instrum.* **13**, 294-297 (1980).

143. Abbas, D. C. & Phelps, D. J. Double-a.c. Hall Effect System with Simple, Digital Oscillator with Application to Semiconductor Measurement. *J. Phys. E: Sci. Inst.* **14**, 1078 (1981).

144. Chu, P., Niki, S., Roach, J. W. & Wieder, H. H. Simple, inexpensive double ac Hall measurement system for routine semiconductor characterization. *Rev. Sci. Instrum.* **58**, 1764-1766 (1987).

145. Kasai, A., Abdulia, A., Watanabe, T. & Takenaga, M. Highly Sensitive Precise Double AC Hall Effect Apparatus for Wide Resistance Range. *Jpn. J. Appl. Phys.* **33**, 4137-4145 (1994).

146. Miranda, P. E. V. d., Coutinho, J. S. F. & Mesquita, A. C. F. Characterization of hydrogen in metallic glasses by the use of Hall effect measurements. *J. Alloys Compd.* **356-357**, 575-578 (2003).

147. Dou, S., Zhang, S., Klein, R. J., Runt, J. & Colby, R. H. Synthesis and Characterization of Poly(Ethylene-Glycol)-Baed Single-Ion Conductors. *Chem. Mater.* **18**, 4288-4295 (2006).

148. Streetman, B. G. & Banerjee, S. *Solid State Electronics Devices* (Prentice Hall, 2000).

149. Michaelson, H. B. The work function of the elements and its periodicity. *J. Appl. Phys.* **48**, 4729-4733 (1977).

150. Dannetun, P., Boman, M., Stafstrom, S., Salaneck, W. R., Lazzaroni, R., Fredriksson, C., Bredas, J. L., Zamboni, R. & Taliani, C. The chemical and electronic structure of the

interface between aluminum and polythiophene semiconductors. *J. Chem. Phys.* **99**, 664-672 (1993).

151. Podzorov, V., Menard, E., Rogers, J. A. & Gershenson, M. E. Hall Effect in the Accumulation Layers on the Surface of Organic Semiconductors. *Phys. Rev. Lett.* **95**, 226601-1-22660-4 (2005).

152. http://www.lakeshore.com/.